METAMATERIAL INSPIRED MULTIFUNCTIOANL ANTENNAS FOR 5G APPLICATIONS

A DISSERTATION

Submitted in partial fulfillment of the
requirements for the award of the degree
of
MASTER OF TECHNOLOGY
in
ELECTRONICS AND COMMUNICATION ENGINEERING
(With specialization in RF & Microwave Engineering)

By

PRIYA SURESH NAIR

(17533014)

DEPARTMENT OF ELECTRONICS & COMMUNICATION ENGINEERING

INDIAN INSTITUTE OF TECHNOLOGY ROORKEE

ROORKEE-247667 (INDIA)

JUNE 2019

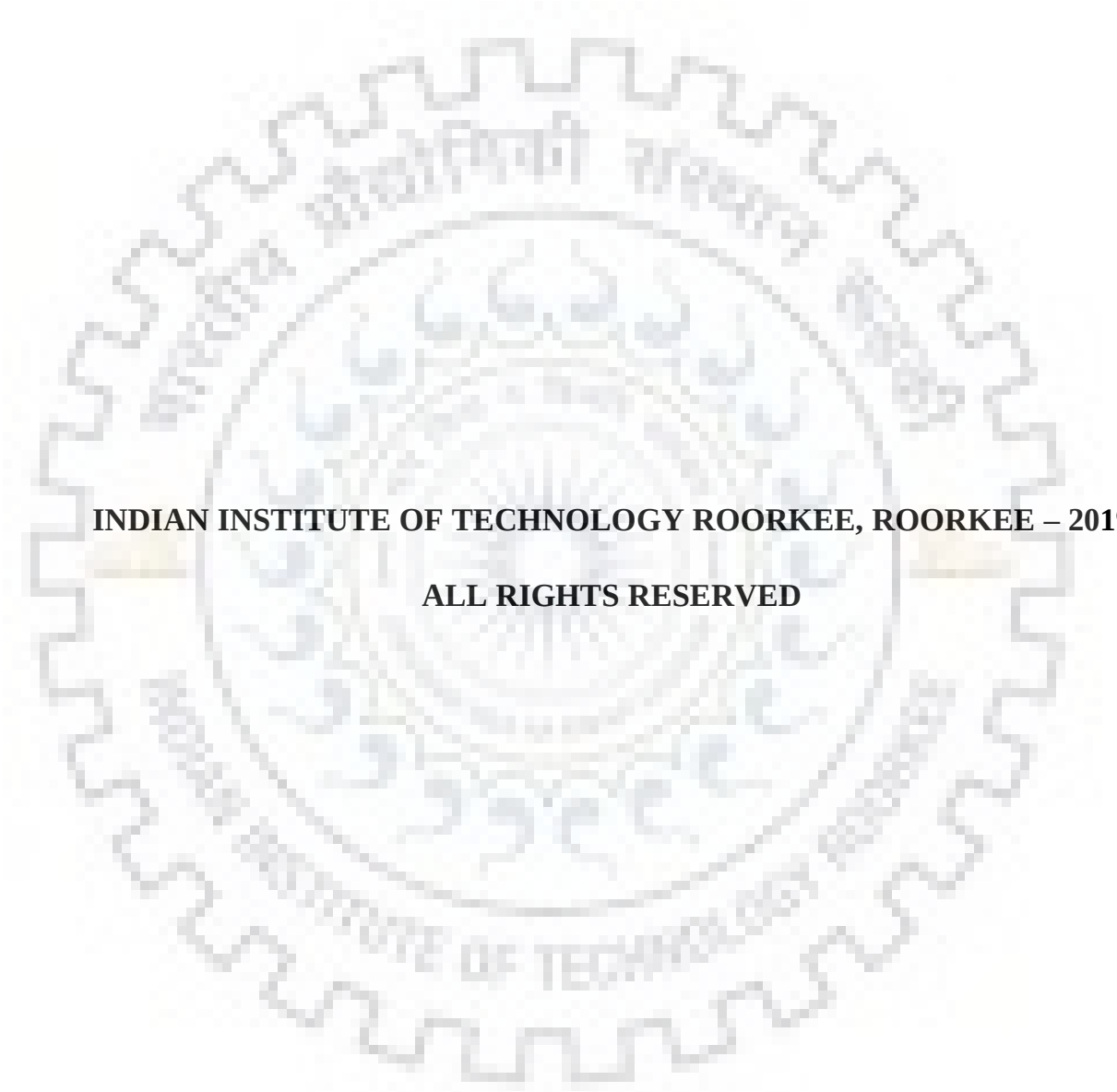

INDIAN INSTITUTE OF TECHNOLOGY ROORKEE

ROORKEE

CERTIFICATE

This is to certify that the dissertation entitled **"METAMATERIAL INSPIRED MULTIFUNCTIONAL ANTENNAS FOR 5G APPLICATIONS"** is a bonafide record of independent work done by **Priya Suresh Nair** (Enrollment No: **17533014**) under our supervision and submitted to Indian Institute of Technology Roorkee in partial fulfillment for the award for **Master of Technology** in **RF and Microwave Engineering.**

SIGNATURE
(Dr. Amalendu Patnaik)
Associate Professor
Dept. of ECE
IIT Roorkee

SIGNATURE
(Dr. M.V. Kartikeyan)
Professor
Dept. of ECE
IIT Roorkee

Date:

Place: Roorkee

INDIAN INSTITUTE OF TECHNOLOGY ROORKEE

ROORKEE

CANDIDATE'S DECLARATION

I hereby declare that the work which is being presented in the dissertation **"METAMATERIAL INSPIRED MULTIFUNCTIONAL ANTENNAS FOR 5G APPLICATIONS"** done by me under the guidance of **Dr. Amalendu Patnaik** and **Dr. M.V. Kartikeyan**, in the partial fulfillment of the requirement for the award of the degree of **Master of Technology** in **RF and Microwave Engineering**, Electronics and Communication Department, Indian Institute of Technology Roorkee, is my original work.

The results submitted in this dissertation report have not been submitted for the award of any other degree or diploma.

Date:
Place: Roorkee

PRIYA SURESH NAIR
Enrollment No: 17533014

Acknowledgements

I feel very privileged in presenting my M-Tech dissertation work in such an authenticable form. I am highly indebted to my supervisors ***Dr.M.V.Kartikeyan and Dr.A.Patnaik***, Professors, Department of Electronics and Communication Engineering, Indian Institute of Technology Roorkee for providing me with the necessary information regarding the project and also for their infilling support in completing the project.

It would not have been possible without the kind of support and help from ***Mr.Sambaiah Pelluri and Ms.Surbhi Adya***, PhD research scholars of the *Millimeter & Terahertz Wave Laboratory*, Indian Institute of Technology Roorkee.I also extend my earnest thanks to ***Dr.S.Yuvaraj***, ***Mr.Debashish Mondal***, ***Mr.Aditya Singh Thakur***, ***Mr.Himanshu Maurya***, ***Ms.Anmol Jain*** and ***Mr.K.Venkateshwara Rao*** whose valuable suggestions and guidance have been helpful in various phases in completion of the project. I am also grateful to all faculty members, my classmates, technical and non-technical staff of Department of Electronics and Communication Engineering, Indian Institute of Technology Roorkee.

I wish to express my heartfelt love and gratitude to my father (***Mr.K.P.Suresh Kumar***), my mother (***Mrs.Bindu P. Nair***) and my brother (***Mr.Priyesh S. Nair***) for their kind co-operation and encouragement which helped me in completion of this project.

Finally, my *pranams* to the almighty for having kept me in peace, good health which paved the way for the successful completion of my M.Tech thesis.

Contents

List of Figures

List of Tables

Chapter 1

INTRODUCTION

Recent years witnessed a growing enthusiasm in artificially engineered structures to develop new, effective and composite materials that replicate the properties not readily available in nature such as negative refractive index, zero phase response etc. Recent examples of engineered material activities include:
1.Metamaterial structures
2.Complex spiral or chiral structures.

1.1 MOTIVATION

Synthesis or construction of metamaterial (MTM) is done by inserting artificially devised inclusions in a specified host medium. The designer is thus provided with a number of independent parameters such as properties of host materials, size, shape and compositions of inclusions. Among these, new possibilities for MTM processing is given by shape of the inclusions. The domain of MTM is providing numerous research and material design opportunities that can be used in various applications[1][2].

It is possible to modify the surface properties of a conductor by incorporating special texture where the assumption is that the period of textured unit cell is considerably low than the wavelength. Such a structure is quantified using a parameter called *surface impedance*. Over the last two decades, abundant work has been done in the area of high impedance surface (HIS) at high frequencies[3].

[12] discusses the results and application of high impedance surface textures over past two decades.

1.2 SCOPE

Engineered textures are being widely used in conjunction with antennas considering their potential to be used at higher frequencies. Metasurfaces are 2D counterpart of metamaterials. They are the most suitable alternative to the traditional optical components. Their main application in the field of antennas is beam steering. They can be used to control amplitude, phase and polarization of the reflected and transmitted EM waves by appropriate modification of the antenna geometry. Other applications of metasurfaces include vortex beam generation, hologram, light bending and focussing etc.

1.3 ORGANIZATION OF THE REPORT

The report work is divided into ten chapters.

- The first chapter provides basic understanding of what are the main topics that are dealt in this report.
- The second chapter describes in detail about metamaterials, its properties, types, classification and how metamaterial based antennas can be classified. It also discusses about the 2D counterpart of metamaterials called *metasurfaces* and its features.
- The third chapter describes a synthetic metal surface called high impedance surface, its unique properties and how these properties help it to act as an excellent substitute to metal ground plane.
- Fourth chapter deals with a latest planar technology called surface integrated waveguide (SIW) that acts as the transformation from non planar to planar technology and its principle of operation is explained. SIW antennas and its types are described in detail.

- Fifth chapter is dedicated to 5G technology that is the beginning to an evolving era in the field of communication. This chapter includes challenges and key features of 5G along with antennas at 5G.

- Sixth chapter is the literature survey done towards this work. It mainly describes the physics behind the design of MTM unit cell, SIW and HIS. The array of unit cells are used to function as an antenna when appropriate excitation and boundary conditions are given. The software used for designing various antennas is also described in this chapter.

- Seventh chapter deals with the discussion of already done works in the field of metamaterial inspired multifunctional antennas at various frequencies under the heading of literature review.

- Eighth chapter deals with the antenna designs that have been simulated using the software called HFSS and the results drawn from it.

- Ninth Chapter lists out the challenges faced during the course of this dissertation.

- Tenth chapter concludes the report followed by bibliography mentioning the references that have been used throughout this dissertation work.

Chapter 2

METAMTERIALS

In 1898, Jagadish Chandra Bose began experiments on twisted structures [31]. Later, in the year of 1914, Lindman did his research on artificial chiral media formed by a collection of randomly oriented small spirals into the host medium [32]. Since then, synthetic materials with complex physics have been the topic of research globally. Fabrication methods of chiral materials have allowed the development of structures that realize qualitatively new, physically realizable response functions that do not occur naturally. And the latest addition to this group is metamaterials (MTMs). Veselago, considered as the father of MTMs, theoretically investigated propagation of plane-wave in a material whose permittivity and permeability were presumed to be both negative [33]. He showed that when a uniform plane wave travels in such a medium, the Poynting vector becomes antiparallel to the direction of the phase velocity [4], contrary to the case of plane wave propagation in traditional media. The experimental verification of such an artificial medium for microwave regime exhibited the presence of unusual refraction [5], opposite to the conventional one.

Interaction of the electric and magnetic moments of the electromagnetic waves with the inclusions of the bulk composite material affects the effective permittivity and permeability on a macroscopic scale. Their values are the basis on which metamaterials are classified.

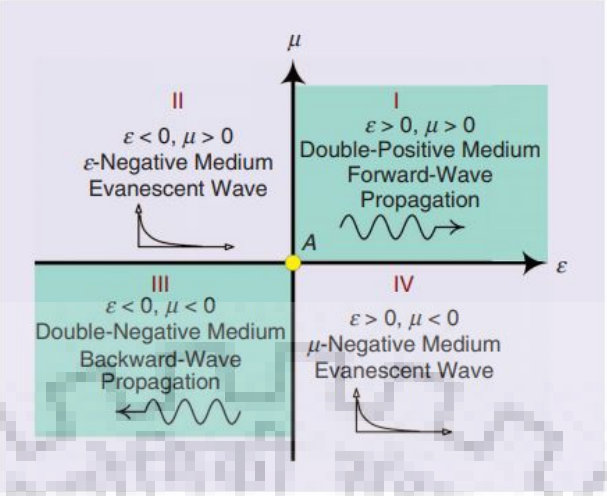

FIGURE 2.1: Metamaterial classification [54]

1.If both permittivity and permeability of the medium are greater than zero (ϵ >0, μ>0), then it qualifies as double positive (DPS) medium. Most of the dielectrics fall under this category.

2.If permittivity is less than zero and permeability is greater than zero (ϵ<0, μ >0), it is called as Epsilon negative (ENG) medium. Plasmas exhibit this behaviour in certain frequency bands.

3.Mu negative (MNG) medium is the one with permittivity greater than zero and permeability less than zero (ϵ >0, μ <0). Some gyrotropic material exhibits this characteristic in certain frequency regions.

4.When both permittivity and permeability are less than zero (ϵ <0, μ <0), such a medium is called Double negative (DNG) medium. This group of materials has been demonstrated with artificial constructs. Several nomenclature and terminologies have been suggested for such kind of materials, such as left-handed, negative refractive index, backward-wave media and double-negative (DNG) metamaterials, to name a few.

In a DNG media, where both ϵ and μ are negative, it has been observed that refractive index has negative real and imaginary parts [34]. Negative imaginary component is the reason for passive nature of DNG media. The following features have been derived from negative index of refraction :

i. phase compensation

ii. dispersion compensation

iii. negative angles of refraction

iv. backward-wave antennas

v. enhanced electrically small antennas

2.1 NEGATIVE INDEX OF REFRACTION

If the wave is travelling in a DPS medium, both the wave vector and the Poynting vector travel in same direction. However, if the medium DNG, where the index is less than zero, the wave vector and Poynting vector are propagating in opposite directions with the later is travelling away from the interface.

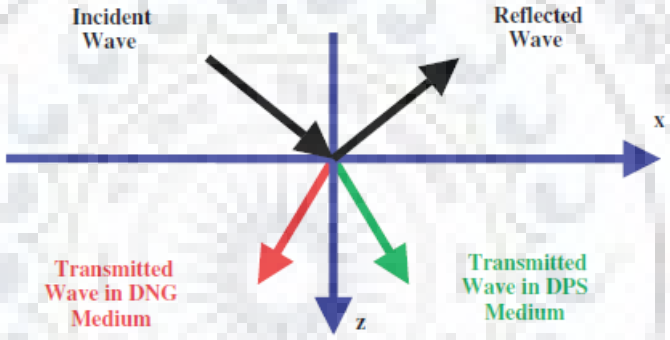

FIGURE 2.2: Effective refractive index [5]

2.1.1 Phase Compensation

An unusual feature of the DNG medium is that it can yield phase compensation, also called phase conjugation. This is due to its property called negative index of refraction [35]. An ordinary lossless slab having positive refractive index n_1 and thickness d_1 and a lossless DNG metamaterial slab having negative refractive index n_2 and thickness d_2 are considered. As this wave travels through the conventional slab, $n_1 k_o d_1$ is the phase difference between the entrance and exit faces. While the total difference in phase between the front and back faces of the ordinary-DNG two-layer structure is $n_1 k_o d_1$ - $n_2 k_o d_2$, indicating that whatever be the phase difference that is created by propagating in the ordinary slab, can be reduced or sometimes, even compensated by traversing through the composite two-structured slab. If, at a given frequency, the ratio $d_1/d_2 = n_2 / n_1$, it can be concluded that

DNG slab can act as a phase compensator since total phase difference is zero between the front-back faces of this composite ordinary-DNG material structure.

2.1.2 Metamaterials having Zero Refractive Index

MTMs having either ϵ and/or μ near zero have index of refraction much less than unity, useful in various applications [1]. The red dot in figure below represents their position on the ϵ-μ space diagram. Several research groups have experimentally materialized planar MTMs that display positive as well as negative refractive index near zero. By achieving matching of resonances in a series-parallel lumped-element circuit, a DNG material at the corresponding frequency can be realized. The propagation constant is a dependent function of frequency that constantly passes through zero (that gives a zero index) with a nonzero slope (that gives a nonzero group speed) in its transition from a DNG to a DPS material. Several applications of these series-parallel MTMs have been proffered and materialized such as couplers, compact resonators, and phase shifters [36 to 41].

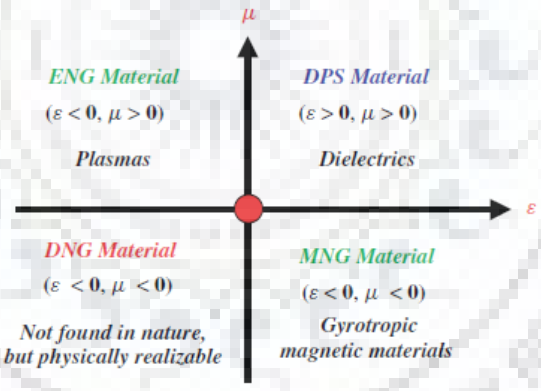

FIGURE 2.3: ZIM at the intersection of different materials[5]

2.1.3 Dispersion Compensation due to DNG Medium

The dispersive nature DNG medium has led to its usage as a *dispersion compensation* tool for various time-domain operations. Dispersion introduces a change in the group speed among various signal components propagating in a DNG medium. By providing dispersion compensation along a transmission line, signals propagating through it would not be distorted. The result being simplification of the components in various devices [51-53]. The main objective is to devise a length

of MTM loaded transmission line that could be integrated with the microstripline to make the combined system dispersionless. The length of the microstripline and MTM loaded transmission line same. In other words, main aim is to fabricate dispersion compensated segment of the transmission line. Therefore the relative ϵ and μ of MTM is designed such that the effective refractive index is equal to that of the refractive index of free space.

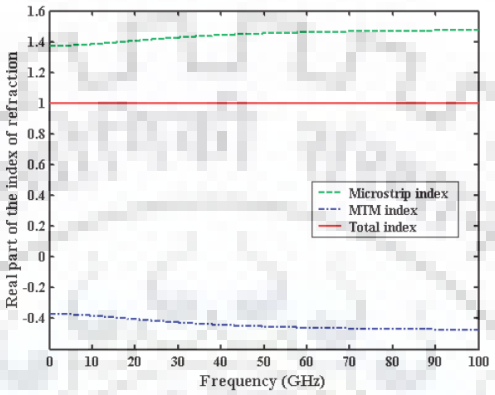

FIGURE 2.4: Refractive index (real part) for different cases [5]

2.2 METAMATERIAL TYPES

Various types of metamaterials are:

- Electromagnetic materials
  - Double negative metamaterials
  - Single negative metamaterials
  - Electromagnetic bandgap metamaterials
  - bi-isotropic and anisotropic metamterial
- Terahertz metamaterials
- photonic metamaterial
- Tunable metamaterials
- Frequency Selective Surface (FSS) based metamaterial

2.3 METAMATERIAL BASED ANTENNAS

Recently many metamaterial based small antennas have been developed. They belong to a class of antennas that use the property of metamaterials to enhance their performance and capability. General classification of MTM based antennas is as follows:

- Leaky wave antennas (LWAs): Guided power leaks away gradually in the form of radiated wave. Composite right or left handed (CRLH) MTM transmission lines are used to realize such antennas. It includes backward to forward beam scanning along with broadside radiation.
- Resonator type small antennas

2.4 HIGH FREQUENCY METAMATERIAL BASED RESONATOR TYPE ANTENNA

Benefits of using MTM based small antennas are:

- compact size
- broad bandwidth
- low cost
- good efficiency

The main reason behind antenna size miniaturization combined with good radiation performance is that the metamaterial manipulates the dispersion relation or near field boundary conditions. *Metamaterials can be used at high frequencies due to the fact the unit cell dimensions are much smaller than the EM wave and they are characterized by antiparallel group and phase velocities* [4] . Antennas based on MTMs make radiation characteristics more controllable.

In this report we will be concentrating on MTM based antennas loaded with metasurfaces such as high impedance mushroom structures (Mushroom HIS) . HIS can

be tuned anywhere between perfect electric conductor and perfect magnetic conductor to achieve good miniaturization factor and optimal bandwidth. Mostly microstrip patch antennas are the ones that are used in conjuction with metamaterials due to their ease of fabrication and low cost. Microstrip patch antennas with MTMs give multiband frequency of operation including L, S, C bands [7].

2.5 METASURFACES

Placing the 3D metamaterial array in a 2D pattern gives a metafilm, which is more often called as ***metasurface (MTS)*** or single layer metamaterial. Individual scatterers that make up each unit cell of this surface are not necessarily having zero thickness. The only condition is that these cells need to be way smaller than the EM wavelength in the surrounding medium. Electric and magnetic polarizabilities of the constituent scatteres define the behaviour of MTS.

2.5.1 Types of MTS

It has two important subclass. They are-

- Cermet topology called ***Metafilms***
- Fishnet topology called ***Metascreens***

Metafilm refers to an array of isolated scatterers whereas metascreen refers to periodically spaced apertures in the surface. Considering the physics behind this surface, it can be modelled using effective-medium theory. It does some kind of averaging of the E and H fields over a given period of unit cell. It is from these averages, the value of ϵ and μ are determined.

Chapter 3

HIGH IMPEDANCE SURFACES

By modifying the structure of conductors, its surface properties can be changed giving rise to another subclass of artificially architectured materials called *high impedance surfaces*. The main boundary condition set for these kind of surface is that the period wavelength is much smaller than the EM wave propagating through it. At many instances in this report, high impedance surface is used in conjunction with *metasurface* as both have same boundary condition that needs to be satisfied to obtain the desired features.

FIGURE 3.1: Cross section of a basic HIS [5]

HIS is generally designed as an array of protruding metallic patches on a planar metallic sheet. It is organized in a 2D framework. Vertical posts connect the metal plates at the top to the planar conductors below. These thumbtacks projecting out from the planar sheet are called *mushroom structures* due to their resemblance to mushroom plant. Top view of the HIS is shown in figure 3.1. The hexagonal shaped metallic patches are projecting above the surface and the connecting vias are represented as dots.

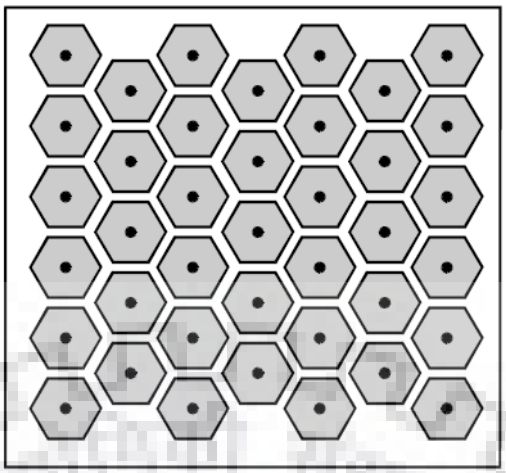

FIGURE 3.2: Outlook of an HIS [5]

HIS can be quantified in terms of lumped circuit elements, essentially capacitors and inductors if and only if the protrusions are smaller than the EM wavelength traversing through it. Capacitive effect is provided by the adjacency of the adjoined metal components whereas inductance is yielded by the lengthy conducting path that associates them together. Effectively, together they act as parallel resonant LC filter that seizes the flow of current through the sheet. The equivalent circuit of HIS is shown below.

FIGURE 3.3: Equivalent impedance model of HIS [5]

HIS exhibits unusual impedance due to which the surface wave modes on this architectured surface are distinctive than those on a conventional metallic ground plane. TM modes that are close to the surface and traverse with a speed that is much less than the speed of light are supported by HIS.

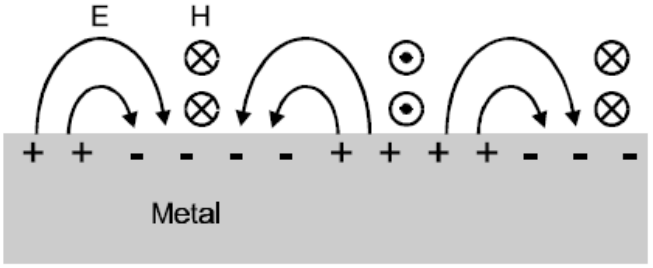

FIGURE 3.4: TM surface waves [5]

It also supports TE modes that only at certain frequencies are restricted to the surface, but radiate readily outside this frequency band. In the case of TE surface waves, both the sheet and the traversing direction of the EM wave are tangential to the electrical field whereas loops of magnetic field stretches out of the sheet.

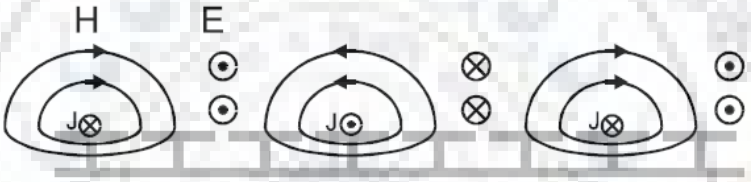

FIGURE 3.5: TE surface waves [5]

It can behave as a magnetic conductor within the frequency range where the surface impedance is large and the tangential component of the magnetic field is small even with a huge electrical field where the surface being considered is approximately lossless. Therefore, it is mentioned as an **artificial magnetic conductor (AMC)**. This condition makes HIS a suitable choice for ground plane in the design of low-profile antennas. A dipole antenna lying flat against an HIS plane will not be shorted out as it would happen with a traditional reflector ground plane because HIS ideally reflects entire power in phase rather than out of phase as done by the metal reflector or conventional ground surface . Hence the radiating element can be positioned adjacent to the surface giving off constructive image current. This in turn enhances efficiency of the antenna. Furthermore the HIS does not support the propagation of surface currents in certain pre-designed frequency band resulting in an improved radiation pattern.

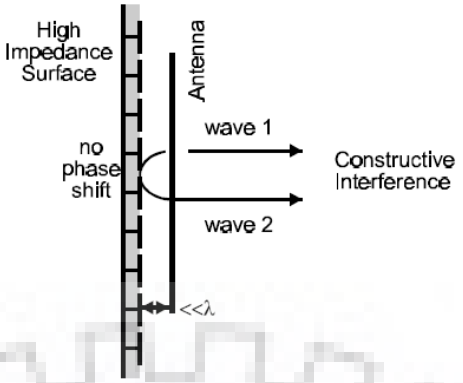

FIGURE 3.6: A flush mounted dipole on an HIS plane [5]

3.1 SURFACE WAVES

Surface waves occur at the interface of heterogeneous materials, for instance metal and free space. In general, surface waves are nothing but travelling EM waves that are restricted between an interface essentially, metal and free space. At optical frequencies, these waves are acknowledged as surface plasmon. Whereas, at microwave frequencies these are no different than the conventional AC currents that exist on the surface of any electricity conducting plane [42-43]. Surface waves do not couple to surrounding plane EM waves in case of a continuous conductor. They radiate if the surface current is scattered by discontinuities such as any bend or textured surface. Surface waves bound to the ground are non-existent on an ideal perfect electric conductor due to infinite conductivity. As a result, the fields that are associated with the surface currents expand into a vast open stretch in space. On a never-ending ground plane, a minute decrement in radiation efficiency acts as a confirmation to the existence of surface currents. They wither away exponentially from the dielectric-metal interface. These waves occur only on interfaces with atleast one component having non-positive dielectric constant such as metals.

In reality, there are only finite sized ground plane through which surface currents travel till they reach a bend or corner. Any discontinuity in surface leads to radiation, or in this case leakage of the currents which results in multipath interference called *speckle*. In case of the far field region, this interference can be visualized as ripples. Undesired mutual coupling occurs among antennas if they share the same ground plane.

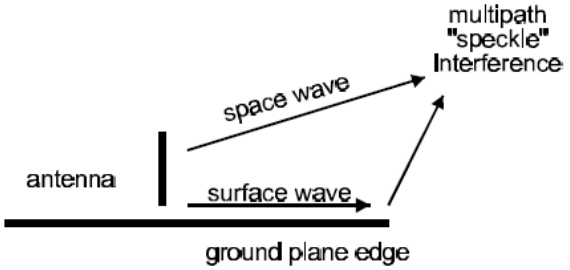

FIGURE 3.7: Multipath interference due to surface waves [6]

3.1.1 Surface Impedance

Surface impedance of an artificial metallic surface is quantified by parallel and resonant L-C circuits. In case of metals, skin depth determines surface impedance. It can penetrate very little into the metal. For instance at a frequency of 10 GHz, Cu has skin depth less than 1 μm. The surface impedance of TM surface wave is given as:

$$Z = j\alpha/\omega\epsilon \tag{3.1}$$

Similarly the surface impedance of TE surface waves is given by:

$$Z = -j\omega\mu/\alpha \tag{3.2}$$

Therefore we can conclude that TM waves require imaginary part of the impedance to be positive, or equivalently need an inductive surface at low frequencies, whereas TE waves require the imaginary part of the impedance to be negative, or a capacitive surface at high frequencies. Close to resonant frequency of the LC equivalent, high surge in surface impedance is seen. In this region, surface waves readily radiate giving rise to leaky waves, instead of being bound at the intersection. Traditional metals slightly show inductive nature, due to the skin effect and as its result back TM waves. Plane metallic surface does not back TE surface waves, whereas dielectric masked metals allow the propagation of TE waves exceeding a certain cutoff frequency. This frequency is dependent on the thickness and dielectric constant of the plane surface.

3.2 ANTENNA DESIGN USING HIS

The main challenge is to design an HIS for a low-profile antenna. The basic structure includes the collection of metallic patches printed on top of a substrate where the patch can have any generic shape. The main properties that make HIS ground plane suitable for low profile antennas are [10]:

- the fact that it can reflect EM waves without phase reversal.
- not supporting surface wave propagation within a certain frequency band.

The most favourable geometry of HIS ground plane is mushroom type as it showcases interesting outputs such as increased directive radiation from a small dipole lying against the ground plane [Ref. Figure 9]. In order to obtain maximum radiation and minimum near field coupling of antenna with the environment, periodic electromagnetic structures are preferred. Multi layer HIS is one such structure [13]. Its architecture consists of dielectric substrate with a ground plane and relatively shifted arrays of electrically small patches which are separated from each other using a dielectric film.

Another method to improve operational bandwidth of HIS ground plane is to reduce cell size. But this leads to narrowband. Therefore a new structure has been proposed that allows unit cell miniaturization as well as bandwidth improvement [14]. [14] also proposes various unit cell geometry and compares them with a parameter R which is defined as percent bandwidth to cell size (in mm^2).

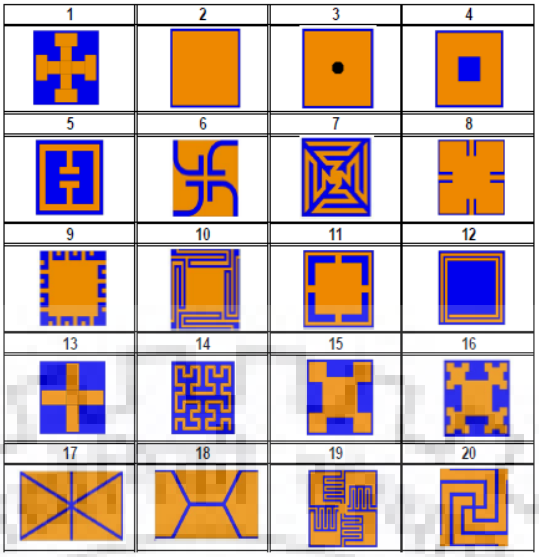

FIGURE 3.8: Various geometries of HIS unit cell [14]

From the above the geometries, interwined ones produce wideband HIS properties for a limited unit cell size. More number of segment arms in the spiral geometry exhibit wider bandwidth.

3.3 ANTENNA ON METAL GROUND PLANE VERSUS H.I.S. PLANE

Consider a metallic ground plane that is finite and bounded. The surface currents produced by the monopole antenna are scattered at any disconinuities present in the plane and at the edges. This causes backward radiation and is the root source of ripples in the main lobe of the radiation or E-H field pattern. In simple words, the direct and scattered radiations from the monopole antenna interfere with each other. The radiation pattern of a monopole at 35 GHz is shown in the figure 3.9. In the figure, monopole has length of 3 mm and area of the metallic ground plane is 5 sq.cm.

FIGURE 3.9: Monopole antenna fed by coaxial cable through a ground plane [5]

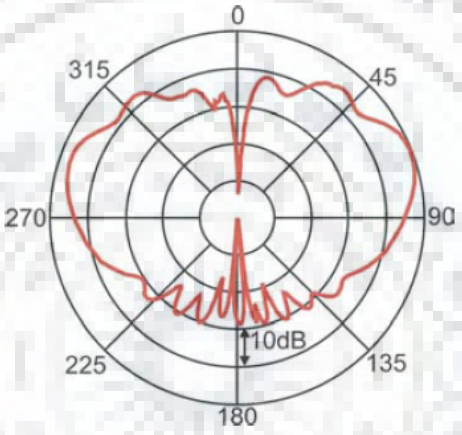

FIGURE 3.10: Radiation pattern of the monopole antenna over a metal ground [5]

Replacing conventional metal ground by an HIS designed at same frequency, suppression of surface waves can be distinctly seen as the radiation pattern becomes more directional. Driven currents are present on any reflective surface as they are conducting. But the driven currents cannot traverse on a high-impedance ground plane. If ever current is induced, it cannot reach the edges of the ground plane as surface currents are confined to the local region all over the antenna. Hence radiation pattern with enhanced directivity and less power in the backward direction is obtained. This is shown in figure 3.12 . This proves that the HIS can be used to minimize the effects of any kind of discontinuity in the ground plane.

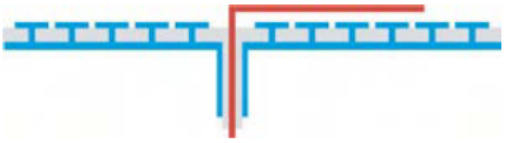

FIGURE 3.11: Low-profile antenna over the HIS [5]

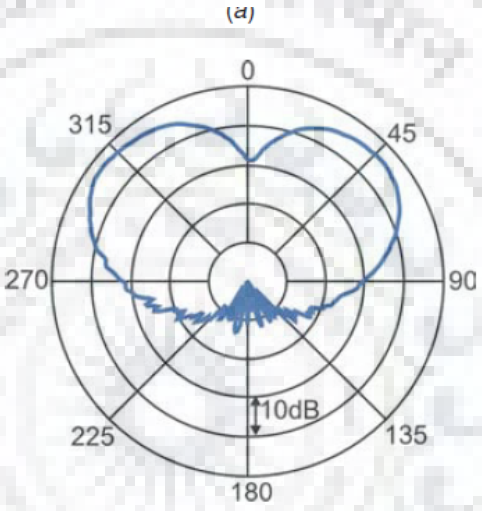

FIGURE 3.12: Radiation pattern of monopole antenna over HIS ground [5]

On comparing the radiation patterns of the monopole antenna without and with HIS, the following features can be noticed. Firstly, there is reduction in central null. This is due to asymmetry in the local geometry. Central null can be regained by introducing symmetry in the geometry. Secondly, reduction in the received power along the horizon because the image currents are reversed on HIS when compared to those on a metal ground. HIS can be used to design various low-profile antennas due to the fact that currents in these surfaces are in phase with the incident EM wave.Antennas with different polarization as well as required directivity can be designed using HIS

Now consider operating the antenna outside the bandgap of HIS. Since surface waves are supported anywhere outside the band, there is a significant difference in the radiation pattern. Figure 3.13 depicts the filed distribution of the same monopole antenna at 26 GHz. Existence of surface waves results in increased

number of side lobes and nulls. Significant power leakage in the backward direction is another disadvantage of surface currents. The case of vertical monopole antenna explains the suppression of surface currents by HIS but it does not signify the importance of the associated unusual reflection-phase property. HIS behaves as a magnetic conductor and since it is artificially textured to attain this property, it is known as ***artificial magnetic conductor (AMC)***. To experimentally verify this, a horizontal wire antenna is fed through the back of the metallic surface through a coaxial cable, as shown in figure 3.11. The wire is bent across the surface and is approximately one-half wavelength long at the resonant frequency of the surface. Placed over a plane and finite metal ground plane, the horizontal wire is shorted out and maximum amount of the power transmitted to the feed is reflected back.

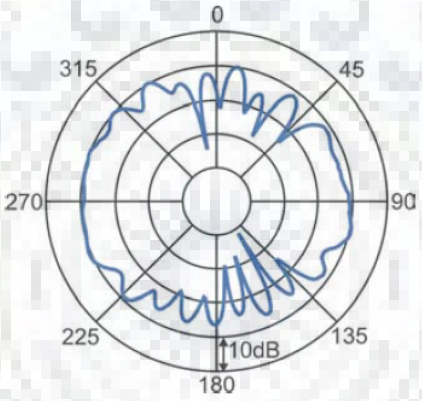

FIGURE 3.13: Radiation pattern of same monopole antenna outside the bandgap [5]

Chapter 4

SUBSTRATE INTEGRATED WAVEGUIDES

At higher frequencies reaching microwave and millimeter wave, ***substrate integrated waveguide (SIW)*** is a blooming technology for the evolution of antennas, circuits and other components. It yields a connective interface between planar and non planar technology. SIW has been associated with the ongoing research and experimental analysis in the domain of millimeter-wave antennas in recent years. It was proposed over one and a half decades ago. It is extensively studied under the category of integrated and efficient transmission lines adaptable to the planar technologies that provides unmatched performances such as self-consistent shielding and large quality factor. It is devised as an open wave-guiding structure. Energy leakage occurs either when the uniformity of these guides is disrupted or when the modes are not excited. This leakage effect is used to design antennas that can radiate in controlled manner by voluntarily introducing disturbances. Having several advantages such as efficiency, broadband and high gain. The main advantage of such an antenna is its compatibility with SIW from which it is derived.

The construction of SIW is done by embedding two rows of metallic vias in a dielectric substrate that are used to bridge the two metal plates between which the dielectric is sandwiched. Traditional waveguides and coaxial lines are non-planar structures which can be converted into planar form by fabricating it with conventional printed circuits such as coplanar waveguide and microstrip lines.

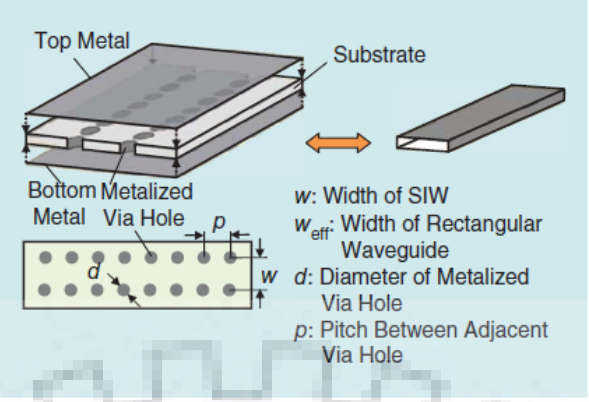

FIGURE 4.1: Structure of substrate integrated waveguide [6]

4.1 PRINCIPLE OF OPERATION

The wave propagation in SIW structures is similar to the propagation in classical rectangular waveguides. The fundamental mode in SIW resembles the TE_{10} mode of a rectangular waveguide. With this mode configuration, the surface current flows along the top and bottom metal planes of the SIW exactly like in a rectangular waveguide, and on the sides it can flow vertically along the metallized surface of the cylinders, being minimally perturbed by the gaps (provided that the gaps are small). For this reason, the electromagnetic field is confined inside the SIW and there is no radiation leakage. This operation mechanism only applies to the TE_{n0} modes of the rectangular waveguide, where the surface current on the side walls flows in vertical direction. For the other modes of the rectangular waveguide, namely TM modes and TE_{np} modes with $p \neq 0$, the surface current across the side walls has a longitudinal component, and consequently it would be strongly perturbed by the gaps. For this reason, these modes are not supported by the SIW structure. In conclusion, the only modes supported by SIW structures are those similar to the TE_{n0} modes of the rectangular waveguide. Due to their geometry and their mode pattern, SIW components can be classified as H-plane waveguide structures [28]. The electric field is normal to the broad wall and its amplitude does not vary in the vertical direction. Moreover, the thickness h of the substrate plays no role in the characteristics of wave propagation, except for conductor losses.

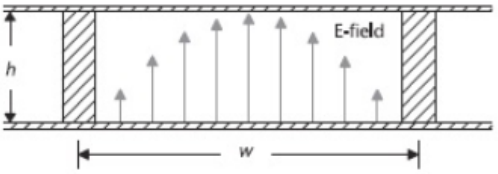

FIGURE 4.2: Electric field pattern of the fundamental TE_{10} in a waveguide[6]

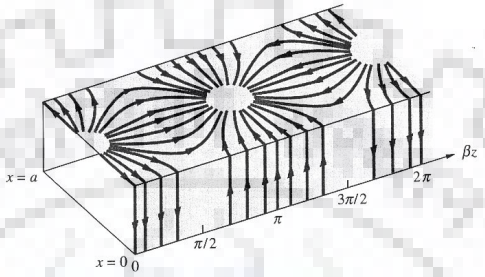

FIGURE 4.3: Surface current flowing pattern of a rectangular waveguide with slots on its sidewalls - TE_{10} Mode[27]

4.2 SIW ANTENNAS

Antennas based on SIW are classied as follows:

- Resonant type
- Non-Resonant type

4.2.1 Resonant type SIW Antenna

Common examples of resonant antennas are microstrip patch antennas and dipole antennas that resonate at discrete frequencies. But in millimeter wave range, these antennas do not provide easy-to-accept performances. They exhibit high conductor losses due high current density at the strip boundaries, more specifically near the feeding network. At higher frequencies, substrate becomes electrically thicker and this leads to the existence of many parasitic surface wave modes. The effect of this phenomena is uncontrolled diffraction of surface waves at the boundaries of the antenna resulting in decreased radiation efficiency and disturbances in radiation pattern. Different antenna designs involving various elements and feeds are

supported by SIW. Slot and patch backed by SIW cavity are the most adaptable antenna designs. To scale down the size of antenna, different techniques are put into use for the design of slot.

Major disadvantage of the resonant structure is that it is narrowband. Further, the radiation efficiency of the microstrip antenna turns out to be less than other types of antennas, with efciencies less than 70%.

4.2.2 Non-Resonant type SIW Antenna

Non-resonant antennas, as the name suggests do not resonate. They are commonly addressed as traveling-wave antennas. Instead of resonating, travelling waves leak energy throughout the path of wave propagation, thereby producing efficient broadband structures. Desired bandwidth and efficiency could be provided by an antenna operating in travelling wave configuration. Under this class of antennas, a traveling wave on a guiding structure acts as the main radiating mechanism. Leakage can be generated under conditions such as enclosed waveguide structures having geometrical asymmetry, open apertures or slots. Therefore, leaky-wave or surface-wave antennas can be developed for millimeter-wave applications including tapered slot antenna (TSA), Yagi-Uda antenna, dielectric rod antenna, long-slot leaky-wave antennas or log-periodic dipole array.

Chapter 5

5G TECHNOLOGY

A remarkable development has been made in the field of mobile and telecommunications. Nowadays, many mobiles have 3G, 2G, bluetooth, WLAN adapters etc [21]. The main focus of 4G was towards the implementation of cellular networks such as GSM and 3G without any technical issues. Security and operating system backing in wireless technologies remain to be tested. 4G has multi mode consumer terminal. The 5G terminals will have software defined radios ,modulation scheme and advanced error-control mechanisms. This improvement is anticipated towards the user terminals as a focus on the 5G mobile networks. The 5G mobile terminals will have access to different wireless technologies at the same time. The 5G terminals would make an ultimate choice among various network providers for a specified service.

5.1 CHALLENGES IN MIGRATION TO 5G FROM 4G

- Software radio approach.
- Consumer Quality of Service (QoS) requirements.
- Security
- Incorporating the current non-IP and IP-based systems into one and providing QoS guarantee for end-to-end services.

- Data encryption

5G technology conceptualizes REAL wireless world or WWWW (world wide wireless web) as it has almost no constraints.

5.2 KEY FEATURES OF 5G

- Offers high resolution and bi-directional bandwidth shaping.
- Implementing subscriber supervision tools for fast action.
- Connectivity speed upto 25 Mbps.
- Supports virtual private network.
- High uploading and downloading speed.

5.3 5G FREQUENCY BANDS

5G spectrum is divided into three main frequency ranges to yield broad coverage and support all user cases. The frequency bands that under consideration for 5G communication are Sub-1 GHz, 1-6 GHz and above 6 GHz [20].

- Sub-1 GHz is aimed to back large scale coverage across rural, suburban and urban regions and help for the benefit of Internet of Things (IoT) services.
- 1-6 GHz offers a good combination of coverage along with capacity benefits. It comprises spectrum within the 3.3-3.8 GHz range that is expected to form the basis for many fundamental and introductory 5G services.
- Above 6 GHz is required to accommodate ultra-high broadband speeds, that is much anticipated feature in 5G. The main focus will be on bands above 24 GHz as this comprises of growing research interest and development in the 24 GHz and/or 28 GHz bands which can be effortlessly implemented together in a composite lone device due to their close proximity. There are also academic interests in analyzing bands within the 6-24 GHz range.

World Radio communication Conference 2019 (WRC-19) plays an important role to implement and achieve the low cost combined with ultra-high-speed vision for 5G devices [20].

5.4 SIW-MTS ANTENNAS AT 5G

Main objective of 5G is to boost transmission bit rates by using frequency bands higher than those already existing bands and widening the signal bandwidth. However, radio frequency loses increases with increase in high frequency bands. The application of massive-element antenna each consisting of more than 100 antennas has been studied as a 5G multiband antenna technology [22]. Application of massive-element antenna makes it possible to compensate for the radio propagation loss by adaptively controlling antenna directivity and increase bit rate by spatial multiplexing of signals.

More attention is given to 5G technology because it is next-gen communication network. As a result more importance is being given to the millimeter (mm)-wave and submillimeter-wave bands. At such higher frequencies, radiation efficiency of an antenna degrades due to considerable metallic and surface wave losses. Introduction of metamaterial based structures, for example metasurfaces or frequency selective surfaces provide better isolation between various antennas in a multi-input multi-output (MIMO) system. MTS block the propagation of surface waves that leads to improved radiation characteristics.

Chapter 6

LITERATURE SURVEY

6.1 MTM UNIT CELL

Metamaterial (MTM) design is generally based on two structures:

- a close-knit bundle of thin wires, giving negative permittivity
- a cluster of split ring resonators (SRRs), giving negative permeability.

6.1.1 Epsilon negative (ENG) materials

An array of parallel wires is shown in figure 6.1. Consider an incident plane wave whose electric field is parallel to the wires. For such a wave, this array exhibits high-pass characteristics.

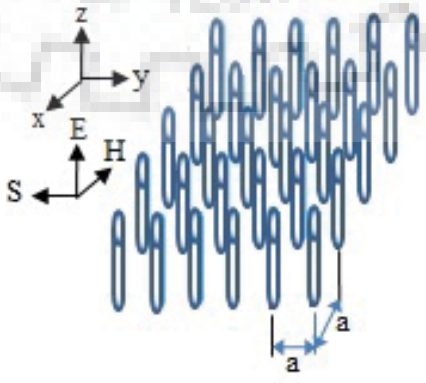

FIGURE 6.1: Array of thin conducting wires [5]

An electromagnetic wave below the cutoff frequency of the array will not propagate through it and undergo total reflection. Similar characteristic is observed when EM waves traverse in plasma. The condition that lattice constant (a) ought to be much smaller than wavelength (a $<<$ λ) of incident wave is satisfied when the wire array behaves as a steady and uninterrupted plasma like material that can be characterized by an equivalent macroscopic relative permittivity with $\omega = 2\pi$ being the angular frequency. Mathematically, it can be denoted as:

$$\epsilon_{\text{reff}} = \epsilon'_{\text{reff}} - j\epsilon''_{\text{reff}} = 1 - {f_p}^2/(f^2 - j\gamma f) \tag{6.1}$$

where

- f, f_p represent the frequency of the signal and the plasma frequency which is the cutoff frequency.
- γ represent losses

The plasma frequency generally depends on the geometry of the system.

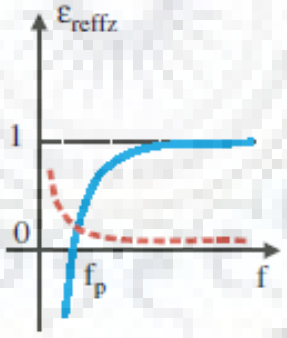

FIGURE 6.2: Effective permittivity [5]

The relative permittivity in the transversal directions (x direction and y direction) is always positive and, in a case of thin wires, is approximately equal to that of the vacuum. The permittivity in the direction parallel to the wires (z direction) also depends on the component of the wave vector in the z direction. Thus the above equation applies only if there is no component of the wave vector in the z direction, that is, if the propagation takes place only in the transversal (xy) plane.

6.1.2 Mu negative Split Ring Resonators (SRRs)

A single split ring resonator (SRR) can be thought of as a small, capacitively loaded loop antenna. If this antenna operates slightly above the resonant frequency, the local scattered magnetic field will be almost out of phase with the incident field. Thus, the resultant local magnetic field will be lower than that of the incident field. It leads to the negative magnetic polarization and negative effective permeability of the resulting metamaterial. It was shown that the effective permeability of this metamaterial has the form given by:

$$\mu_{\text{eff}} = \mu'_{\text{eff}} - j\mu''_{\text{eff}} = 1 - ({f_{\text{mp}}}^2 - {f_{\text{o}}}^2)/(f^2 - {f_{\text{o}}}^2 - j\gamma f) \tag{6.2}$$

where

- f is frequency of the signal
- f_{mp} is magnetic plasma frequency at which μ_{eff}=0
- f_o is the resonant frequency of SRR at which μ_{eff} diverges.

An array of split ring resonators is shown in figure 6.3. This configuration has been extensively used for the construction of MNG materials. The SRR is anisotropic in nature. When the incident plane wave has magnetic field vector perpendicular to the SRR, the induced currents yield negative permeability. Contrarily, when the magnetic field vector is along or parallel to the SRR, there are no induced currents and therefore the effective permeability is not affected by the presence of the SRR.

FIGURE 6.3: Array of circular geometry SRRs [6]

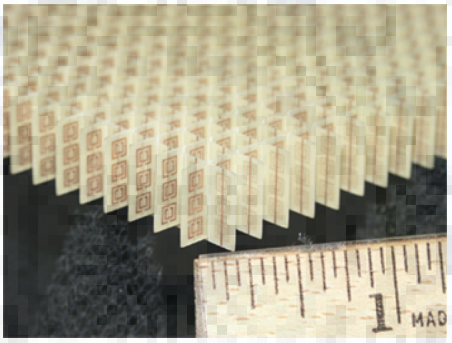

FIGURE 6.4: Array of square geometry SRRs [6]

From this we can conclude that MTMs allow backward-wave propagation provided the condition that magnetic field vector perpendicular to the SRRs is satisfied. To achieve nearly isotropic 2D MNG material characteristics, atleast two SRRs per unit cell must be utilized.

6.1.2.1 DNG Metamaterial - Combination of thin wires and SRRs

Early design of DNG metamaterial was merger of the thin-wire-based epsilon negative structure and the SRR-based mu negative element as shown in figure 6.5. It was expected that the new compound material showed a macroscopic effective permittivity equal to that of the thin-wire ENG medium and a macroscopic effective permeability identical to the permeability of the SRR-based MNG medium.

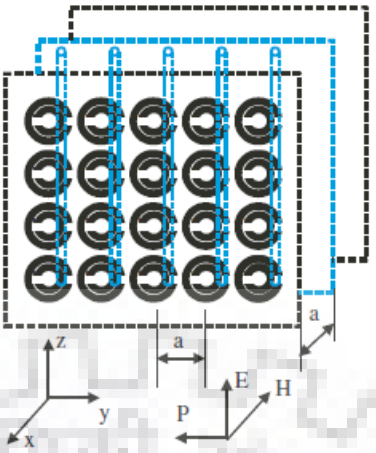

FIGURE 6.5: DNG MTM element based on the combination of thin wires and SRRs [5]

6.2 HIS DESIGN PARAMETERS

If frequency of operation and bandwidth are given, HIS design procedure is as follows:

i. for two layer structure as shown below:

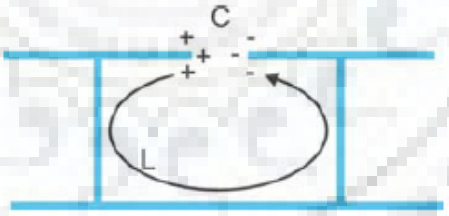

FIGURE 6.6: Two layer structure of HIS [5]

The fringing electric fields between adjacent metal patches is used to model the capacitors. For such fringing capacitors, the capacitance value can be approximately determined as:

$$C_{\text{fringe}} = \omega(\epsilon_1 + \epsilon_2)/\pi + arccosha/g \tag{6.3}$$

where

- a is lattice constant

- ω is width of plates
- g is gap between the plates
- ϵ_1 is the dielectric constant of the substrate
- ϵ_2 is the dielectric constant of the surrounding medium, which in most cases is free space.

ii. for three layer structure as shown below:

FIGURE 6.7: Three layer structure of HIS [5]

For a given thickness, capacitive loading is used to achieve lower resonant frequency. According to this geometry, the top two overlapping layers introduce the parallel-plate capacitors' effect. The capacitance is calculated with the help of a well-known equation as given below:

$$C_{\text{parallel}} = A\epsilon/d \tag{6.4}$$

where

- ϵ is the dielectric constant of the substance between the plates
- d is the separation between the plates.
- A is the surface area of the plates

In either of the above two cases, sheet capacitance value is determined by the value of the individual capacitors and a geometric factor F that depends on the selection of lattice:

$$C = C_{\text{individual}}F \tag{6.5}$$

where

- F=1 for a square lattice
- F=$\sqrt{3}$ for a triangular lattice

- F=$1/\sqrt{3}$ for a hexagonal grid etc.

The inductance of an HIS is determined absolutely by its substrate thickness. This can be experimentally verified by using a solenoid of current that involves two rows of plates and the vias associated with them. The vias are placed across the capacitor. Current flows up through one row of vias and comes down through the next set of vias to the ground plane.The length and width of the solenoid are neglected to determine the sheet inductance. The formula used for sheet inductance is:

$$L = \mu t \tag{6.6}$$

where

- μ is the permeability of the substrate
- t is the thickness of the material

for a given frequency ω_o and bandwidth B_w we can calculate thickness as:

$$t = cB_w/\omega_o \tag{6.7}$$

6.3 DESIGNING SIW STRUCTURES

The field pattern within an SIW structure is comparable to that of a conventional rectangular waveguide. The design of any SIW structure begins with defining the waveguide width for the required frequency band and available substrate. Therefore, the equivalent width of the SIW is an important and initial design parameter. [18] presents a new method based on the mode-matching technique (MMT) for the modelling the actual SIW width 'a_{SIW}', expressed in terms of the equivalent waveguide width 'W'. This W determines the frequency range and bandwidth of the SIW. Reflections from an all-dielectric waveguide of width 'W' to an SIW of width 'a_{SIW}' forms the basis for this method. If this is the least reflection, then the actual SIW width is best adjusted to the equivalent waveguide width. Other two important design parameters are 'p' and 'd' i.e. the pitch between two vias and the diameter of the vias, respectively. For practical purposes, d/p ratio

varies between 0.5 and 0.8. Provided cutoff frequency [f_c], dielectric constant of the substrate [ϵ_r] and d/p ratio, we can calculate 'W' as follows:

$$W = c/2f_c\epsilon_r \tag{6.8}$$

From which we can 'a_{SIW}' as:

$$a_{SIW} = W + p[(0.766e^{0.4482d/p}) - (1.176e^{-1.214d/p})] \tag{6.9}$$

6.4 ANSYS HFSS SOFTWARE

HFSS stands for ***High Frequency Structure Simulator***. It is a 3D EM simulation software that is used in the design and simulation of high frequency structures such as antennas, RF or microwave components such as filters, connectors, IC packages etc. It is the software used for the antenna design throughout this dissertation work. It is based on *Finite Element Method* (FEM) computational technique. It is preferred over other EM simulators due to its ease of use and accuracy in the results. In this procedure a structure is subdivided into many smaller subsection called finite elements. The finite elements that is used by HFSS are tetrahedron and the entire collection of this tetrahedron is called mesh.Next, solution is found for the fields within each finite element and these fields are interrelated so that they satisfy Maxwell's equations throughout the structure. This provides field solution for the overall original structure. Once this field solution is obtained, matrix solution is determined. Few advantages of HFSS include the presence of field calculator, 3D layout meshing etc. among many others.

6.5 METAMATERIALS BASED ANTENNA

Few of the latest works in the field of antennas inspired by MTMs are as follows:

- Development of the antennas based on metamaterial structures such as zero-phase-shift line, composite left/right-handed, zero-index, mushroom, and high permittivity periodic structures [9]. In this paper feeding of mushroom like structure has been simplified.

- Multi-band MTM based microstrip antennas are designed for WLAN and WiMAX applications [8]. This paper gives the two methods that are good for multiband performance and they are etching slots on the patch and loading of shorted pins and walls.

- A compact multiband MTM based microstrip patch antenna for wireless communication applications [7]. Traditional microstrip patch antenna covers only L and S bands whereas metamaterial based antennas cover L, S and C bands. As gain of the antenna is increased, its size decreases.

6.6 HIGH IMPEDANCE SURFACES

- A new wideband and compact HIS [14] suggests how to use his to reduce antenna thickness. It also shows how the reflection phase changes from -180^o to +180^o. The phase reflection is zero at resonant frequency.

- Design and analysis of multilayer high impedance surface [13] gives reason why antenna size must be compact for electronic designs as well as how multilayer HIS structure improves the antenna performance.

- High-Impedance Surfaces with aperiodically-ordered textures [10]. Application of arificial magnetic conductor for low profile antennas is discussed in this paper.

6.7 SIW ANTENNAS

- SIW antennas and arrays [15] give a detailed analysis of different antennas configurations such as slot, leaky wave, dipole, log periodic antennas etc. It also discusses the critical issues faced during the manufacturing of antenna array using SIW technology.

- A new switched beam antenna array working at 26 GHz for future 5G application is discussed in [25]. It is based on the sub-arrays consisting a combination of different slot shapes (L,U,S) integrated in Substrate Integrated Waveguide (SIW). The phase shift between each slot is achieved by varying the location of these slots [25].

6.8 SIW BASED ANTENNA FOR 5G COMMUNICATION SYSTEMS

[23] provides a basis for the construction of an SIW based vivaldi antenna structure. Gibson created vivaldi antenna in 1979 [26] and it is widely used due to its innat properties such as minimal cross-polarization, broad bandwidth and large gain. An eight element antenna array within 40.5 to 43.5 GHz band is considered. The authors discuss and experimentally demonstrate how beamforming can achieved by a narrow-beam in E-plane but a wide-beam in the H-plane. The structure and optimal design of this antenna is given in the paper[23].

FIGURE 6.8: Fabricated vivaldi antenna [23]

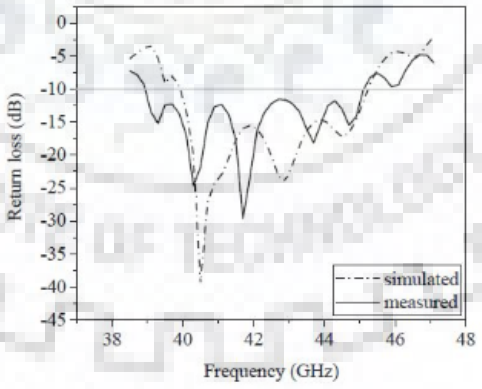

FIGURE 6.9: Simulated and measured return loss of antenna [23]

Measured results show that the operating frequency band of the proposed antenna is from 38.9 GHz to 45.1 GHz, where the relative bandwidth is 14.76 %) within S_{11} < -10 dB. Measured results approach the simulated result and covers the desired band. This proves the usefulness of vivaldi antenna arrays for 5G applications.

Chapter 7

ANTENNA DESIGNS

7.1 MILLIMETER WAVE SIW ANTENNA FOR 5G APPLICATIONS

The design of a linearly polarized substrate integrated waveguide (SIW) antenna operating at a frequency of 54 GHz is proposed with references taken from [29]. Gain achieved is approximately 7.1 dBi. Introduction of slots in the basic SIW cavity design affects its resonant frequency and impedance bandwidth. TE_{104} is the chosen mode as the frequency band under considered is very high. The substrate used is RT/Duroid 3003. The simulation is carried out in ANSYS HFSS and only simulation results are presented.

The slot locations were decided based on the eigen mode analysis of the SIW cavity. Eigen mode analysis gives accurate field maxima and minima. The slots are introduced in the places of maximum electric field. Maximum radiation takes place though these slots, thereby enhancing the directivity and gain. Slots are also helpful in designing low profile antennas. To overcome the limitations of impedance matching in a wide frequency range at millimeter wave bands, the combination of tapered profile and SIW technology is implemented.

7.1.1 Design Structure

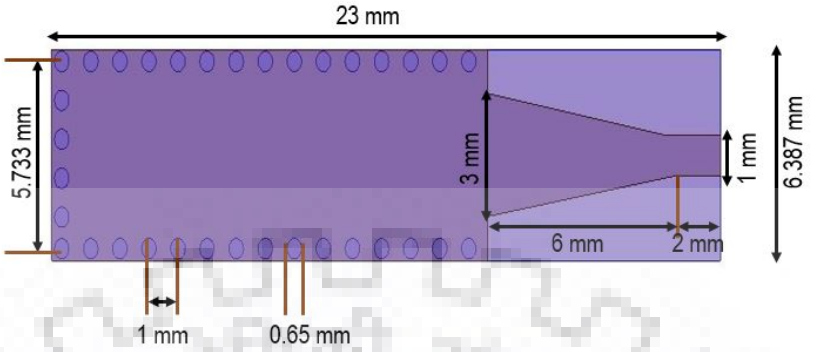

FIGURE 7.1: SIW cavity geometry

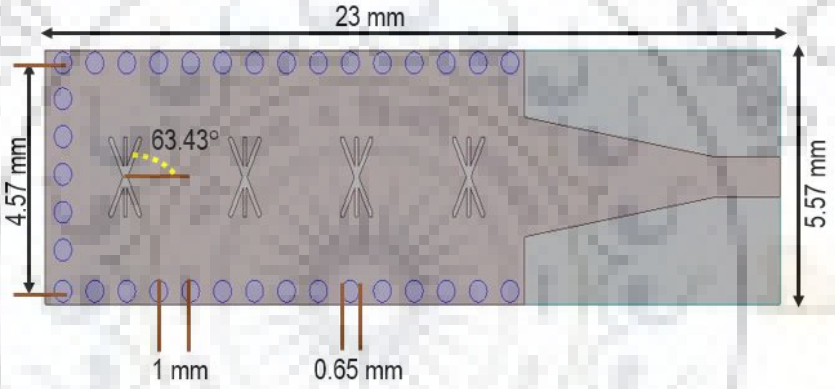

FIGURE 7.2: Antenna design values with slots

7.1.2 Design Parameters:

TABLE 7.1: Cavity design parameters

Design Parameters	**Numerical Values** (mm)
Substrate length	23
Substrate width	6.387
Substrate thickness	0.508
Effective width of SIW	5.733
Diameter of the vias	0.65
Pitch	1
Length of the tapered section	6
Width variation of the tapered section	3 to 1
Length of the constant width micro strip	2

- Material used: RT/Duroid 3003
- Loss tangent: 0.0013
- Relative permittivity: 3

TABLE 7.2: Antenna design parameters

Design Parameters	**Numerical Values** (mm)
Substrate length	23
Substrate width	5.57
Substrate thickness	0.508
Effective width of SIW	4.57
Diameter of the vias	0.65
Pitch	1

7.1.3 Simulated Results

All the simulations were carried out by the ANSYS HFSS software that uses finite element method (FEM) computational technique. The value of S_{11} for the cavity design was found to be -17.5517 dB. Value of the reflection coefficient, S_{11} is reduced to -22.5 dB and the antenna size is reduced with the introduction of slots. It is also observed that with the proper slots positioning the antenna can also be made dual band. The graph shows a dip at 56.4 GHz but the insertion loss is -13 dB which has a scope for improvement. The simulated radiation pattern of the design is as shown below. The proposed design achieves a sufficiently good gain of 7.1032 dBi.

TABLE 7.3: Parameters achieved in HFSS after simulation

Design Parameters	**Numerical Values**
Peak directivity	6.1644
Peak gain	5.6605
Radiation efficiency	91.826%

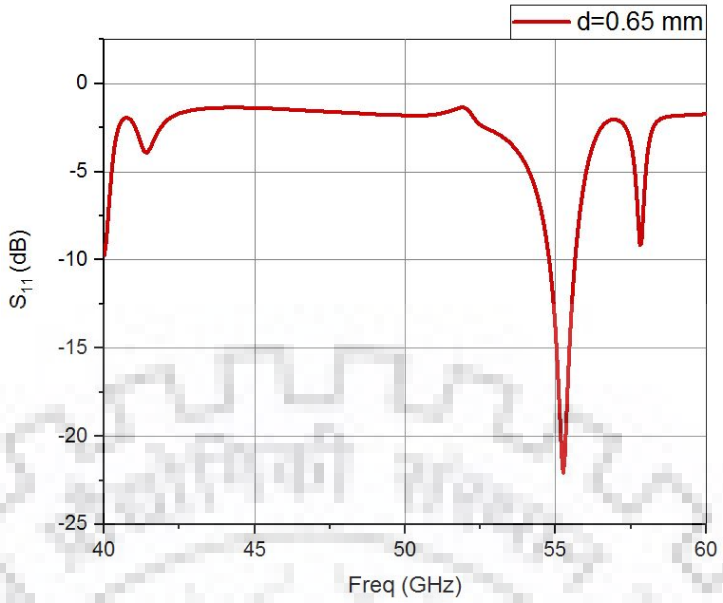

FIGURE 7.3: Reflection coefficient of SIW antenna with slots

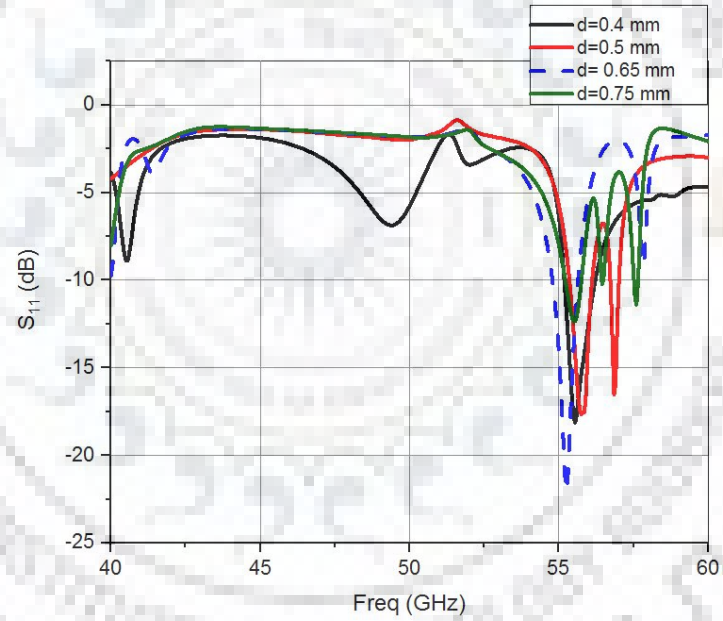

FIGURE 7.4: Parametric study of SIW antenna by varying diameter of vias

7.1.4 Derived Conclusion

This work presents a design that can find a potential application in 5G communication. The antenna is low-profile and providing good parammetric results, eventhough there is scope of improvement in this design. The paper mainly focuses on the introduction of slots to attain antenna miniaturization and decent gain with good efficiency.

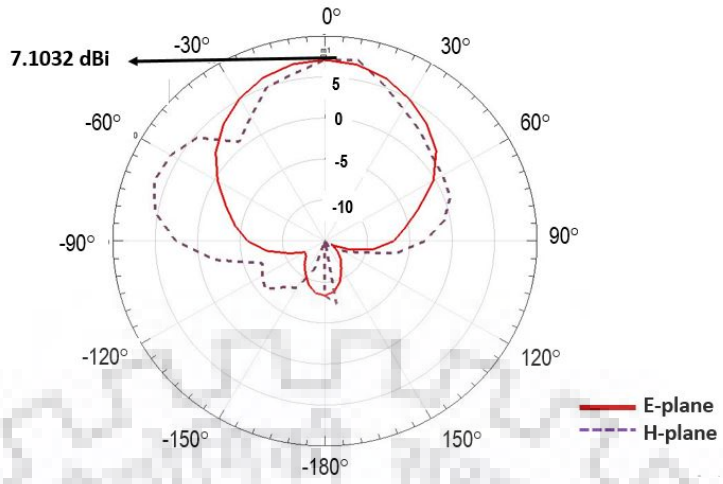

FIGURE 7.5: Radiation pattern of the proposed design

7.2 SIW CAVITY BACKED BOW-TIE SLOTTED ANTENNA OVER METASURFACE TO IMPROVE FTBR

Traditional rectangular slots in an antenna gives narrowband response. This is the reason for selecting bow-tie shaped slot to obtain a wider bandwidth response. The frequency band chosen for this design in 8-12 GHz, with operating frequency being 10 GHz. This antenna is placed over a simple HIS-mushroom metasurface with rectangular patches connecting the conductive layer below through vias. The distance between the antenna and MTS is 25mm. It helps in improving ***Front to Back Ratio***, FTBR and maintain it at 18.27 dBi. This is 3 dB more than the acceptable value at 5G frequency band. The simulated results give maximum peak gain of 4.33 dBi and an efficiency 87.9%. Substrate used is RT/Duroid 3003 with the height of substrate being 0.75 mm.

7.2.1 Design structure

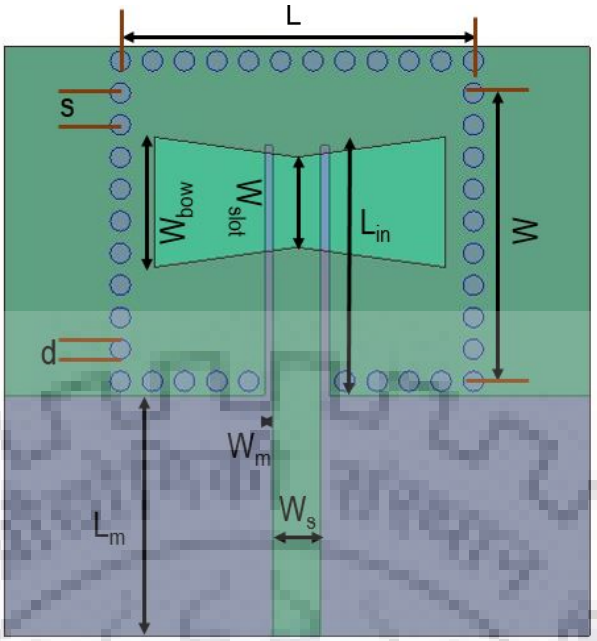

FIGURE 7.6: SIW cavity backed Bow-Tie slotted antenna geometry

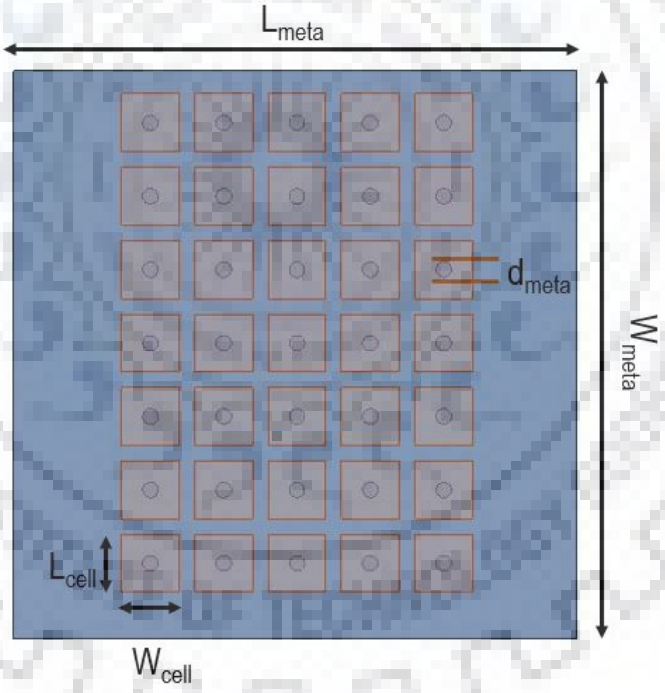

FIGURE 7.7: Square shaped mushroom MTS geometry

7.2.2 Design parameters

- Material used: RT/Duroid 3003
- Loss tangent: 0.0013
- Relative permittivity: 3

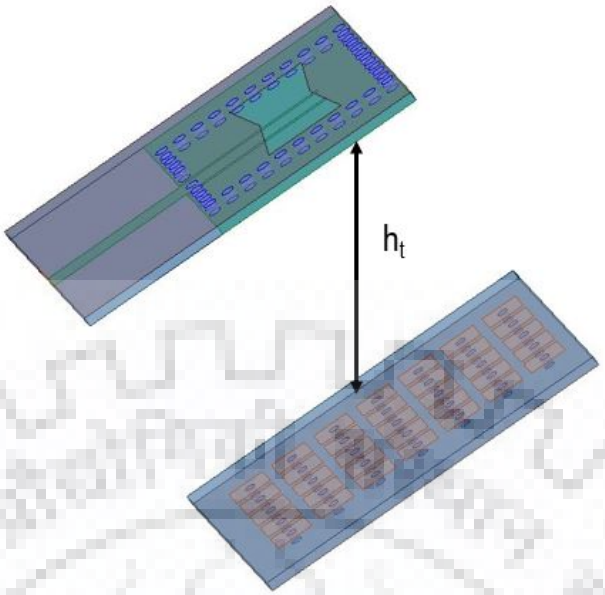

FIGURE 7.8: Bow-Tie slotted antenna over MTS arrangement

TABLE 7.4: Bow-Tie Antenna design parameters

Design Parameters	**Numerical Values** (mm)
Substrate length (L)	17.6
Substrate width (W)	16
Substrate thickness	0.75
Diameter of the vias (d)	1
Pitch of the vias (s)	1.6
Length of slot (L_{slot})	14.5
Inner width of slot (W_{slot})	4.5
Outer width of slot (W_{bow})	6.5
Inset feed length (L_{in})	12.5
L_m	12
Feed width (W_s)	2.4
Inset feed slot width (W_m)	0.4

7.2.3 Simulated results

The initial dip at 9.89 GHz in the S_{11} plot is due to TE_{101} mode. Without the bow-tie, the resonant frequency for TE_{102} mode is at 14.7 GHz [37]. With the introduction of bow-tie slot, the resonant frequency of TE_{102} mode is shifted to a lower frequency of 10.32 GHz. This shift causes the broadening of the frequency band that was otherwise, narrowband. With the introduction of metasurface under the antenna at a height of 25mm, the FTBR has improved from 12 dB to 18.27 db.

TABLE 7.5: Mushroom MTS design parameters

Design Parameters	**Numerical Values** (mm)
Metasurface length (L_{meta})	29
Metasurface width ($_{meta}$)	29.4
Diameter of connectors (d_{meta})	0.4
Length of each cell (L_{cell})	3
Width of each cell (W_{cell})	3
Distance between MTS and Bow-tie antenna (h_t)	25

This is an acceptable value for 5G communication. As the FTBR has improved, the directivity and subsequently the gain of the antenna has also increased.

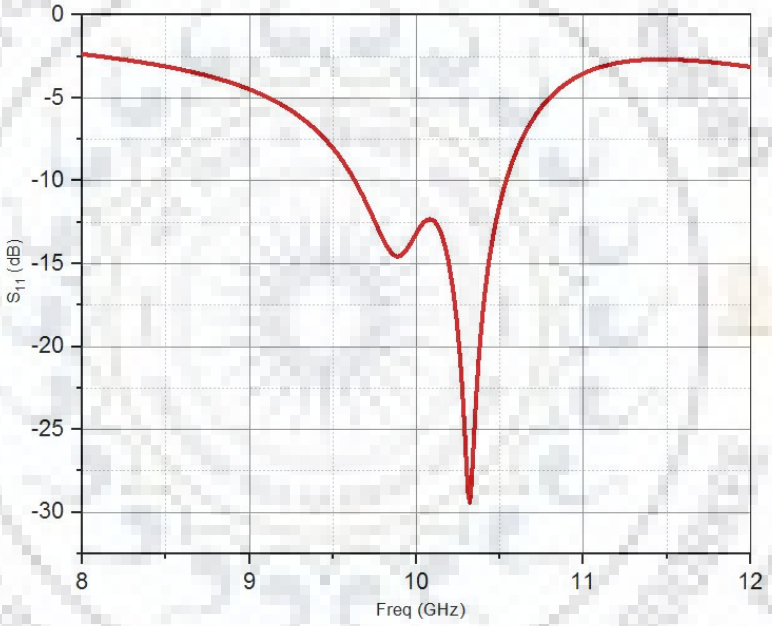

FIGURE 7.9: Reflection loss of the antenna with MTS

TABLE 7.6: Parameters achieved in HFSS after simulation

Design Parameters	**Numerical Values**
FTBR	18.7 dB
Peak gain	4.9 dB
Radiation efficiency	87.6%

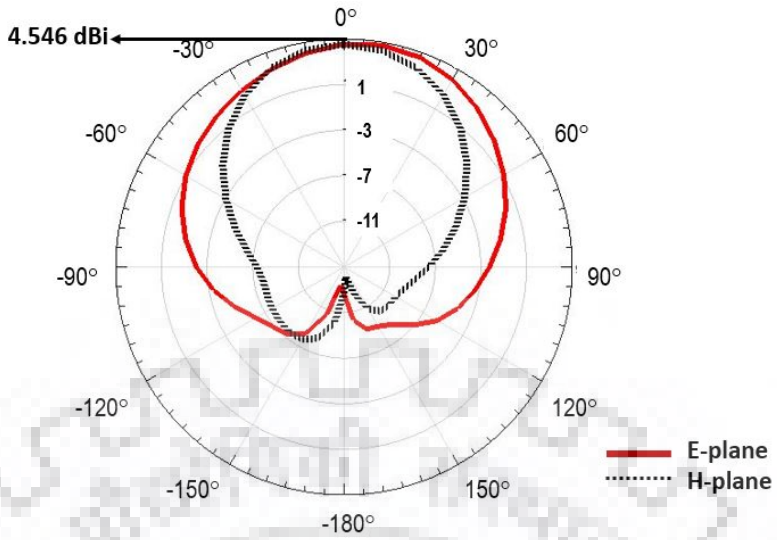

FIGURE 7.10: Radiation pattern of the antenna with MTS

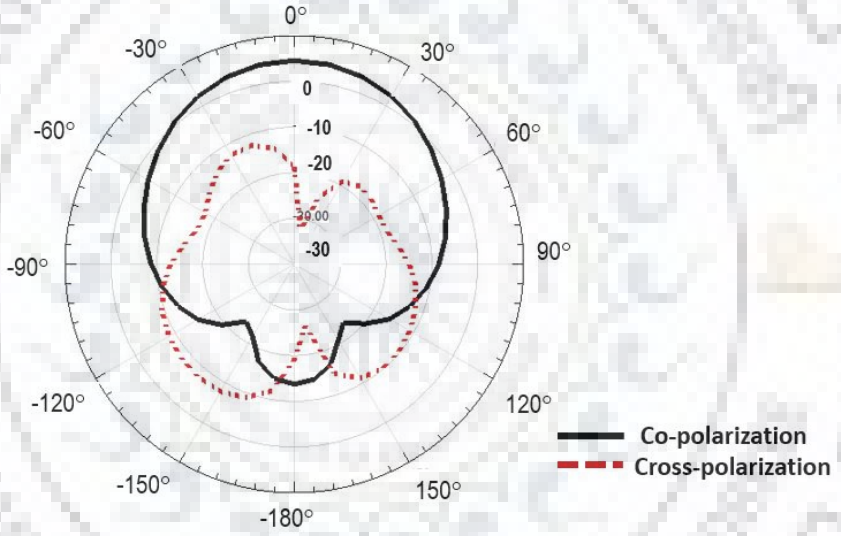

FIGURE 7.11: Co and cross polarization the antenna with MTS

7.2.4 Conclusion derived

The introduction of bow-tie slot instead of conventional rectangular slot has improved the bandwidth of the antenna. The mushroom-MTS has improved the directivity and finally the gain of the antenna to 4.5 dBi. It also enhanced the FTBR of the antenna to 18.27 dB when compared to the antenna with plain metallic ground plane. The antenna has achieved an efficiency of 87.9% and is found to be a suitable antenna design in 5G communication systems.

7.3 MILLIMETER WAVE DUAL-BAND SIW ANTENNA FOR 5G APPLICATIONS

This work proposes a linearly polarized substrate integrated waveguide (SIW) antenna operating within a frequency band of 40 GHz-60 GHz. The paper shows how the introduction of HIS-mushroom metasurface helps to reduce back side radiation and thus improve directivity. $\mathbf{TE_{104}}$ is the mode under consideration as frequency band chosen is high. The substrate used is RT/Duroid 3003 with copper coating having height equal to 17 um. The simulations are carried out using the software ANSYS HFSS. Only simulated results are present.

The HIS-mushroom structure is the most basic and simple example of a high impedance surface. It improves directivity by seizing the surface current flow in the frequency band of interest and by reflecting the incident EM waves without phase reversal.

7.3.1 Design structure

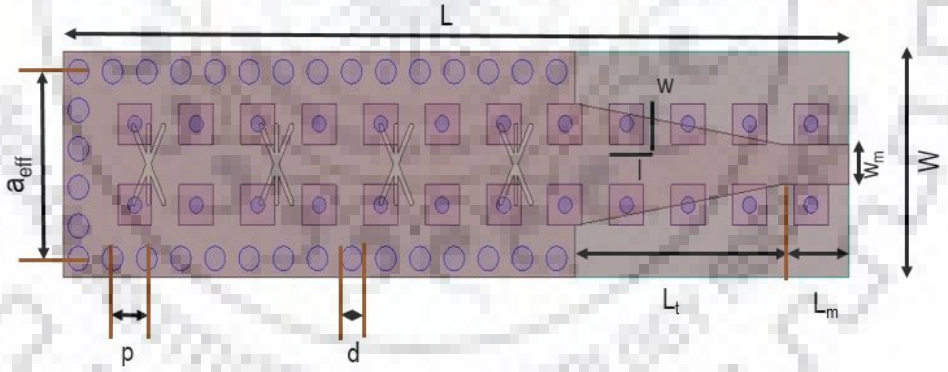

FIGURE 7.12: Antenna geometry with slots and EBG metasurface

7.3.2 Design parameters

- Material used: RT/Duroid 3003
- Loss tangent: 0.0013
- Relative permittivity: 3

TABLE 7.7: Antenna design parameters

Design Parameters	**Numerical Values** (mm)
Substrate length (L)	23
Substrate width (W)	5.57
Substrate thickness	0.508
Effective width of SIW (a_{eff})	4.57
Diameter of the vias (d)	0.65
Pitch of the vias (p)	1
length of EBG unit cell (l)	1
width of EBG unit cell (w)	1
Length of the tapered section (L_t)	6
Width of microstrip (w_m)	1
Length of the constant width micro strip (L_m)	2

7.3.3 Simulated results

All the simulations were carried out by the ANSYS HFSS software that uses finite element method (FEM) computational technique and only simulated results are presented. The value of S_{11} for the cavity was found out to be -17.5517 dB. The S_{11} values of the SIW cavity backed slot antenna is as shown in the graph below. The dual-band is obtained as a result of the positioning of the slots in the design. The E-plane and H-plane radiation patterns of the antenna are also simulated that show the gain obtained is around 7.8 dBi with enhanced directivity and efficiency. This is appreciable value considering the losses that occur at 5G frequencies.

TABLE 7.8: Parameters achieved in HFSS after simulation

Parameters	**55 GHz**	**57 GHz**
Peak directivity	6.8	6.5
Peak gain	8.08 dBi	7.95 dBi
Radiation efficiency	94.1%	93.98%

7.3.4 Conclusion derived

This work presents an antenna design for possible application in 5G communication. The not so explored frequency band of 5G spectrum has been used as many research works have already investigated the 24 GHz-28 GHz band. The

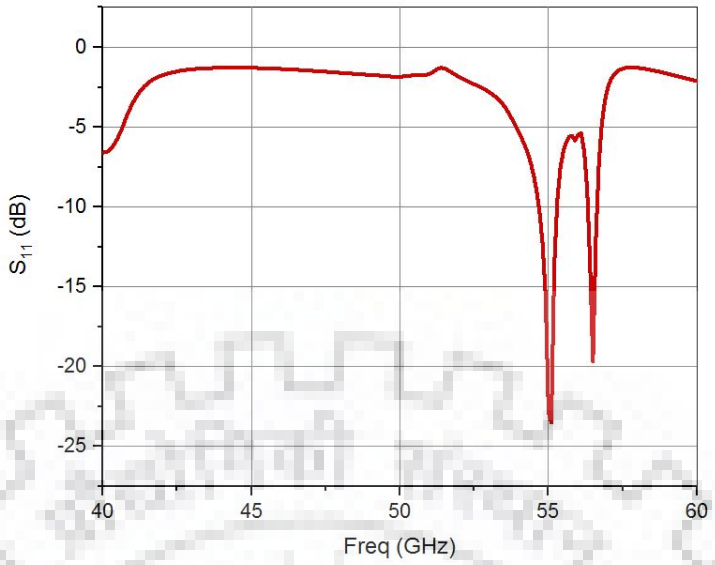

FIGURE 7.13: Reflection loss of the antenna

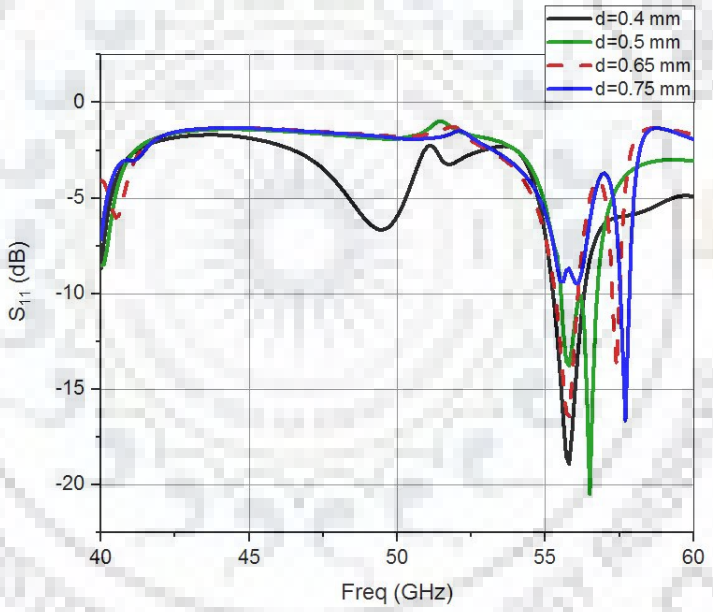

FIGURE 7.14: Parametric study of the antenna by varying the diameter of vias

paper mainly focuses on how the SIW cavity backed slot antenna is utilized to realize a planar antenna geometry at very high frequency band, 40 GHz- 60 GHz. This antenna provides substantial gain and efficiency satisfying the quantitative measurements that are expected from an antenna operating at 5G. The improved directivity is achieved due to the use of HIS-mushroom metasurface. Only simulated results are present as the equipments for fabrication and testing of antenna at such high frequency are under order.

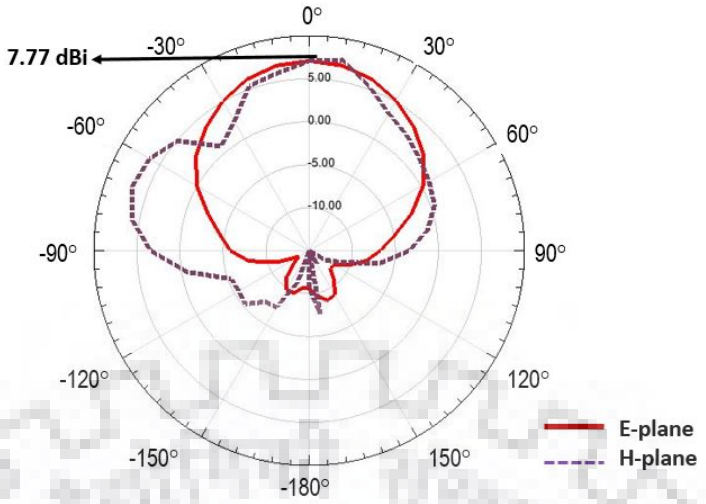

FIGURE 7.15: Field pattern of the antenna at 55 GHz

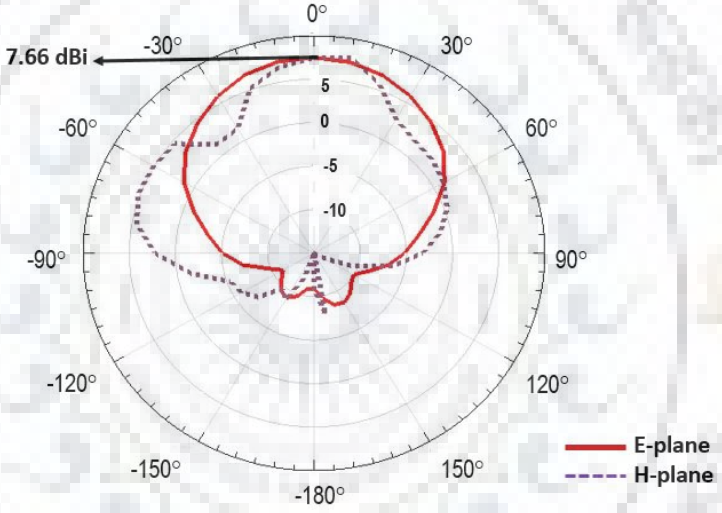

FIGURE 7.16: Field pattern of the antenna at 57 GHz

7.4 MULTI-BAND SIW ANTENNA WITH MODULATED METASURFACE AT 5G FREQUENCY

A multi-band SIW antenna which is linearly polarized is designed. The antenna consists of a T-shaped radiator inscribed on the upper side of the dielectric substrate [32]. This radiator is responsible for multi-band occurrence. The operating frequency is chosen to be 24 GHz, which is a valid selection for 5G applications. An aperiodic modulated metasurface is employed as the ground plane for the proposed antenna. Modulated MTS is a great alternative to the metal ground as it enhances the gain and subsequently the front to back lobe ratio (FTBR) of the antenna [31]. The substrate used is FR4 epoxy with a thickness of 0.8 mm. The

simulations are done using ANSYS HFSS. Only simulated results are presented as the antenna fabrication is under process.

The reason for calling it modulated MTS because change in size of the unit cell is resulting in a change of the output gain and resonant frequency. Modulated MTS antenna is an excellent alternative to conventional high gain antennas or antenna arrays. It also yields beneficial features like low-profile antenna and ease of fabrication etc. that makes it a suitable device for 5G applications. These kind of antennas make use of interaction between MTS and surface wave. The MTS is designed such that its surface impedance is spatially modulated. This modulation can be achieved by varying length, width, height, material etc. of each unit cell. Here the length and width of each element within a unit cell.

7.4.1 Design structure

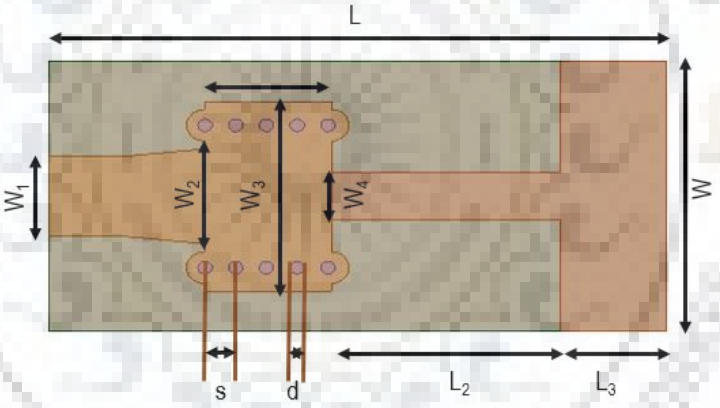

FIGURE 7.17: T-radiator SIW antenna with dimensions

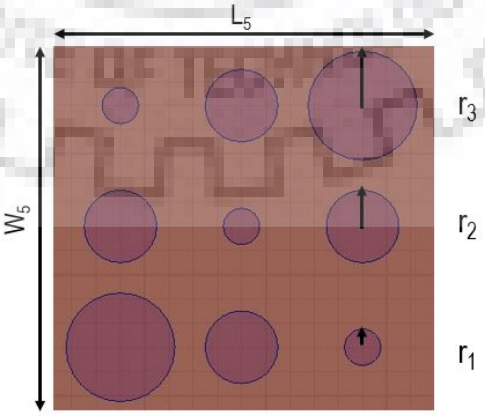

FIGURE 7.18: Geometry of modulated MTS unit cell

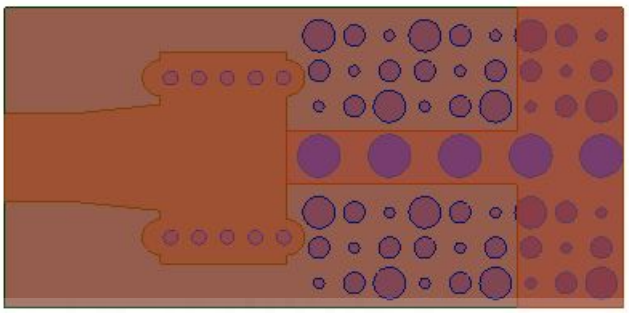

FIGURE 7.19: T-radiator SIW antenna with modulated MTS

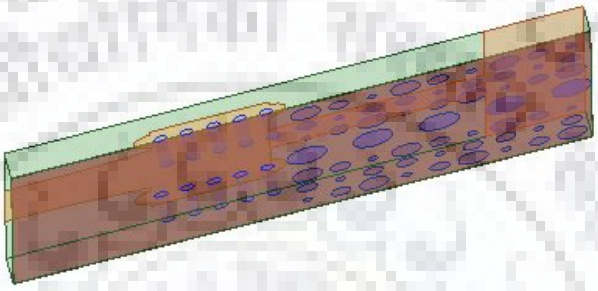

FIGURE 7.20: Side view of T-radiator SIW antenna with modulated MTS

7.4.2 Design parameters

- Material used: FR4 Epoxy
- Loss tangent: 0.02
- Relative permittivity: 4.4

7.4.3 Simulated results

From the graph in figure 8.12, it can be clearly stated that the introduction of modulated metasurface results in decreased reflection loss. The multi-band occurrence is due to the T-radiator etched on the upper side of the FR4 epoxy substrate.

Gain of the antenna without modulated MTS is about 3 dBi [32] whereas gain of the proposed antenna with modulated MTS is 4.92 dBi. Therefore it is seen that the increase in gain is about 2 dBi with the replacement of conventional metal ground with modulated aperiodic MTS. Therefore the proposed antenna is an efficient radiator with decreased back lobe and increased gain.

TABLE 7.9: Antenna design parameters

Design Parameters	**Values** (mm)
Substrate length (L)	17.5
Substrate width (W)	8.5
Substrate thickness (th)	0.8
Length of SIW (L_1)	3.6
Width of SIW (W_3)	6
Diameter of the vias (d)	0.4
Pitch (s)	0.8
Width variation of tapered section (W_1-W_2)	2.5 to 3
Length of first part of T-radiator (L_3)	3
Length of second part of T-radiator (L_2)	6.5
Width of T-radiator (W_4)	1.5
Radii of circular patches (r_1, r_2, r_3)	0.15,0.3,0.45
Length of AMC unit cell (L_5)	3.1
Width of AMC unit cell (W_5)	3.1

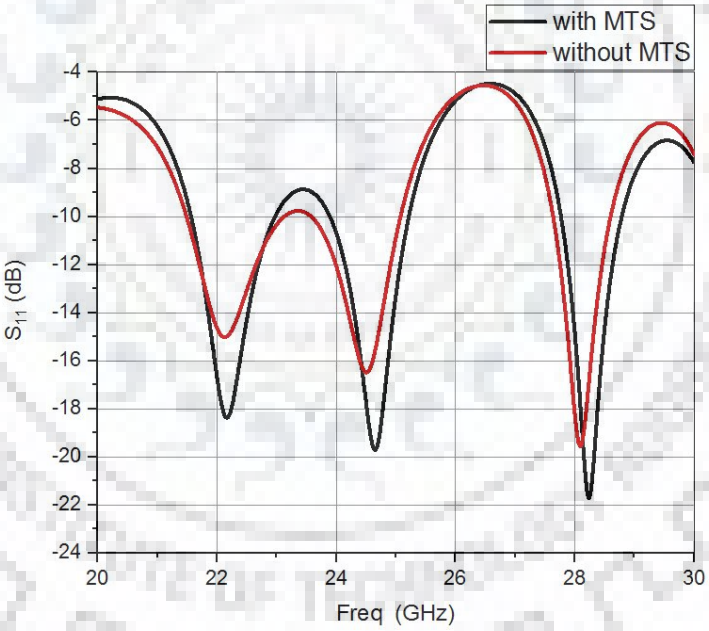

FIGURE 7.21: Parametric study: Reflection coefficient of T-radiator SIW antenna with and without MTS

7.4.4 Conclusion derived

The introduction of modulated aperiodic metasurface (MTS) improves gain of the antenna by 2 dBi and also enhances the FTBR of the antenna when compared to the antenna with metallic ground plane. This is clearly visible in the radiation pattern simulated using HFSS as shown in figure 8.13. The presence of

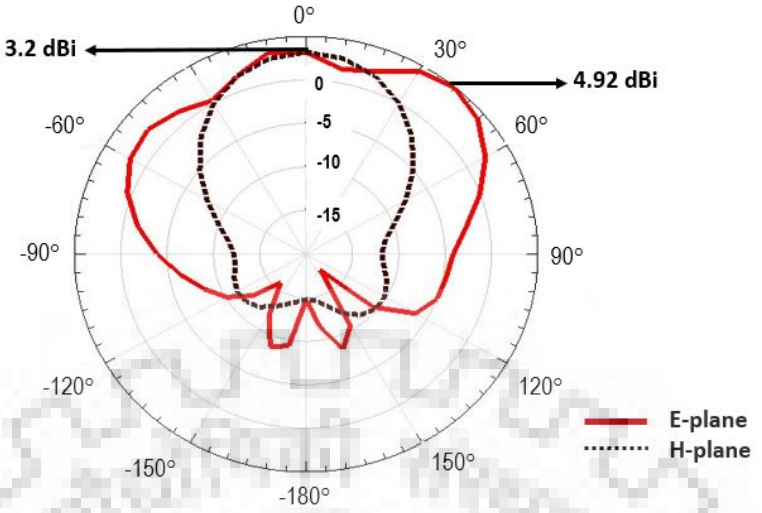

FIGURE 7.22: E and H-plane fields at 24 GHz

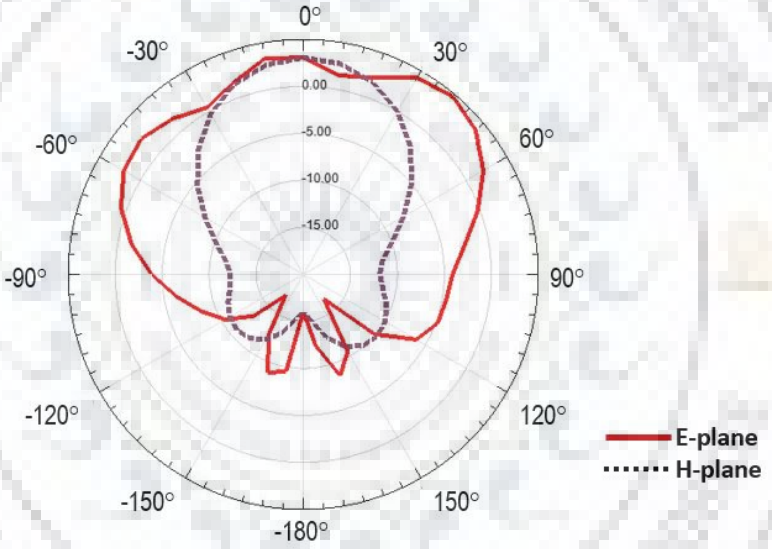

FIGURE 7.23: E and H-plane fields at 22 GHz

T-radiator in the antenna design is responsible for multi-band existence and SIW along with tapered microstrip feeding ensures low reflection loss over a wide range of frequency.

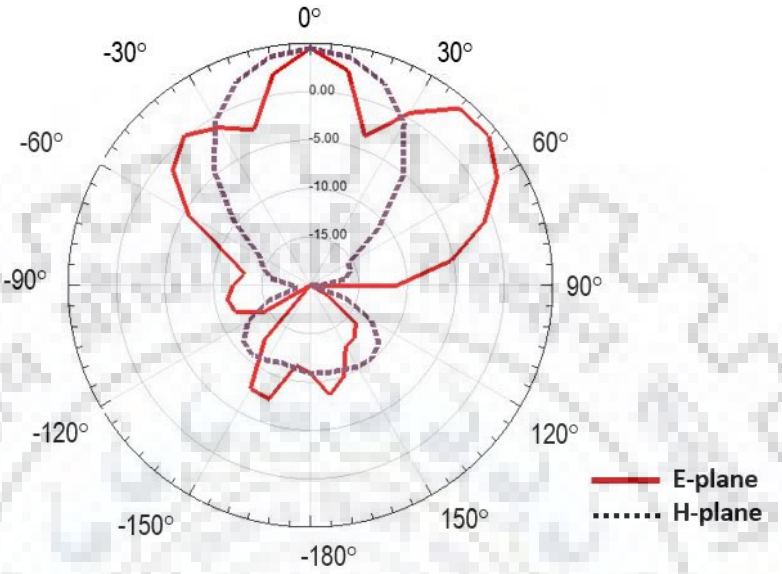

FIGURE 7.24: E and H-plane fields at 28 GHz

TABLE 7.10: Parameters achieved in HFSS after simulation

Design Parameters	**22 GHz**	**24 GHz**	**28GHz**
Peak directivity	5.5	5.4	6.7
Peak gain	4.85 dBi	4.92 dBi	4.87 dBi
Radiation efficiency	85.6%	84.6%	83.6%

Chapter 8

CONCLUDING REMARKS

8.1 PUBLICATIONS

- ***Publication Accepted:*** "Multi-Band SIW Antenna with Modulated Metasurface at 5G Frequency" by ***Priya Suresh Nair***, Amalendu Patnaik and M.V.Kartikeyan at IEEE Indian Conference on Antenna and Propagation (InCAP) 2018 in Hyderabad- Published.
- ***Publication under Pipeline:*** "Millimeter Wave Dual-Band SIW Antenna for 5G Applications" by ***Priya Suresh Nair***, Amalendu Patnaik and M.V.Kartikeyan at IEEE WINTECHCON-2019 : Technical Conference by Women in Engineering- Communicated.

8.2 NOVELTY OF THE WORK

The main objective of this work was to show the importance of metasurfaces in 5G antenna technology. I have used metasurfaces as well as modulated metasurfaces to show how they can be used in enhancement of antenna parameters such as directivity, gain, radiation efficiency and FTBR. I have tried to incorporate the parametric values of all the four designs that have been done towards the fulfillment of this dissertation.

8.3 OUTLOOK AND FUTURE SCOPE

Through this dissertation work, importance of artificially engineered structures to enhance the antenna performance has been analyzed. Metamaterial based antennas perform well for high frequency applications because of its boundary condition that the size of the unit cell must be very small when compared to the EM wavelength. Under MTMs, there comes metasurfaces and high impedance surfaces. Metasurfaces provide the same characteristics as that of metamaterials but with reduced surface area. In present day scenario where reduction in physical size is an important consideration, MTS is the best alternative to MTM in antenna design. High impedance surfaces are proven to be better ground plane reflectors when compared to conductive reflectors as they reflect the entire power without phase reversal and hence a small dipole antenna lying against HIS ground plane will not short out. Substrate integrated waveguide technology is one which transforms non planar to planar structures and hence allows easy PCB fabrication. SIW antennas and arrays have gained high popularity in recent years due to the fact that wireless communication systems have open an era for the implementation of extremely compact and unified systems. It is also discussed how these structures can be used to manufacture antennas that need to work at high frequencies welcoming the 5G technology. The main aim of this dissertation work is to design low-profile antennas for 5G communication. The software used in simulating designs throughout research work is HFSS (*High Frequency Structure Simulator*) by ANSYS. The computational technique used by the software is Finite Element Method (FEM). This software is preferred over other simulation softwares due to its accuracy and user-friendly nature.

This work consists of four antennas designed at various 5G frequency bands. Their quantitative parameters such as peak directivity, gain, radiation efficiency and polarization have also been mentioned. The reflection coefficient plot gives a detailed analysis on the impedance matching of the designed antenna. Its radiation pattern and co-cross polarization plots provide information about its peak directivity and peak gain. Antenna fabrication is done using LPKF machine that uses PCB technology.

This work has a lot of potential to be researched upon. The following lists out the future scope of my work.

- Developing new designs for massive MIMO, which is considered the most suitable for 5G antenna technology.
- Developing MTS based antennas to act as polarizers.
- Introduction of H.I.S. in filter-antennas.
- Work on aperiodic nature of AMC and how it can be used to improve radiation characteristics of massive MIMO.

Bibliography

[1] Christophe Caloz and Polytechnique Montreal,*"Ten Applications of Metamaterials"*, 2016 IEEE International Symposium on Antennas and Propagation (APSURSI)

[2] T.J.Cui, R.Liu and D.R.Smith,*"Metamaterials: Theory, Design, and Applications"*, New York: Springer Science, 2010.

[3] Theofano Kollatou and Christos Christopoulo,*"Use of High-Impedance Surfaces in Electromagnetic Compatibility Applications"*, IEEE Transactions on magnetics, VOL. 45, NO. 3, MARCH 2009

[4] Christophe Caloz and Tatsuo Itoh*"Metamaterials for High-Frequency Electronics"*, IEEE invited paper

[5] Nader Engheta and Richard W.Ziolkowski,*"METAMATERIALS:Physics and Engineering Explorations"*, John Wiley & Sons, 2012

[6] *"www.researchgate.com"*

[7] Nikhil Kulkarni and G.B.Lohiya,*"A Compact Multiband Metamaterial based Microstrip Patch Antenna for Wireless communication Applications"*, Int. Journal of Engineering Research and Application, Vol. 7, Issue 1, (Part -1) January 2017, pp.01-05

[8] Kai Yu, Yingsong Li and Yanyan Wang,*"Multi-Band Metamaterial-Based Microstrip Antenna for WLAN and WiMAX Applications"* , 2017 International Applied Computational Electromagnetics Society Symposium - Italy (ACES)

[9] Zhi Ning Chen, Xianming Qing, Jin Shi, Nasimuddin and Wei Liu,*"Metamaterial-based Antennas: Engineering Designs"*, 2015 Asia-Pacific Microwave Conference (APMC)

[10] Ilaria Gallina, Alessandro Della Villa, Vincenzo Galdi, Vincenzo Pierro, Filippo Capolino, Stefan Enoch and Gerard Tayeb,*"High-Impedance Surfaces with Aperiodically-Ordered Textures"*,Electromagnetics in Advanced Applications, 2007.

[11] F.Linoty, R.Cousinz, X.Begaud and M.Soirony,*"Design and Measurement of High Impedance Surface"* , Proceedings of the Fourth European Conference on Antennas and Propagation, April 2010

[12] S.Kildal, A.Kishk and S.Maci,*"Artificial Magnetic Conductors, Soft/Hard Surfaces, and other Complex Surfaces"* , IEEE Trans. Antennas and Propagation, vol. 53, No. 1, Guest Eds., 2005

[13] P.Saleem Akram and Dr.T.Venkata Ramana *"Design and Analysis of Multi layer High Impedance Surface"*, International Journal of Engineering Research and Technology (IJERT) Vol. 2 Issue 10, October 2013

[14] Anthony Bellion and Mickael Cable*"A New Wideband and Compact High Impedance Surface"*, IEEE 15th International Symposium on Antenna Technology and Applied Electromagnetics, June 2012

[15] Pampa Debnath and Sayan Chatterjee,*"Substrate Integrated Waveguide Antennas and Arrays"*, 2017 1st International Conference on Electronics, Materials Engineering and Nano-Technology (IEMENTech)

[16] Caroline Sebastian, V.J. Amirtha Vijina, Ramesh R. and Usha Kiran K.,*"The Design of High Gain Substrate Integrated Waveguide Antennas"*, IEEE International Conference on Wireless Communications, Signal Processing and Networking (WiSPNET) 2016

[17] Sunil Dwivedi, Prof Divyanshu Rao and Prof Ravi Mohan,*"Substrate Integrated Waveguide Based Leaky-Wave Antenna"*, International Research Journal of Engineering and Technology (IRJET) Volume: 03 Issue:02, Feb-2016

[18] Zamzam Kordiboroujeni and Jens Bornemann,*"Designing width of substrate integrated waveguide structures"* , IEEE Microwave and wireless components letters, VOL. 23, NO. 10, October 2013

[19] Xiao-Ping Chen and Ke Wu,*"Substrate Integrated Waveguide Filter"*, IEEE Microwave magazine, July/August 2014

[20] *"5G Spectrum Public Policy Position"*, Copyright of 2016 GSM Association, November 2016

[21] Asvin Gohil, Hardik Modi and Shobhit K Patel,*"5G Technology of Mobile Communication:A Survey"*, IEEE 2013 International Conference on Intelligent Systems and Signal Processing (ISSP)

[22] Satoshi Suyama, Tatsuki Okuyama, Yuki Inoue and Yoshihisa Kishiyama,*"5G Multi antenna technology"*, 5G laboratory, research laboratory NTT DOCOMO

[23] Pengfei Liu, Xiaowei Zhu, Xiang Wang and Ling Tian,*"A SIW-Based Vivaldi Array Antenna for 5G Wireless Communication Systems"*,IEEE International Symposium on Antennas and Propagation & USNC/URSI National Radio Science Meeting, July 2017

[24] Reshma S.Sapakal and Sonali S.Kadam, *"5G Mobile Technology"*, International Journal of Advanced Research in Computer Engineering & Technology (IJARCET) Volume 2, Issue 2, February 2013

[25] Xu F. and Wu K., *"Guided-Wave and Leakage Characteristics of Substrate Integrated Waveguide"*, IEEE Trans on MTT; 2005, 53: 66-73

[26] P.J.Gibson, *"The Vivaldi Aerial*, in Proc. of the 9th European Microwave Conf., 1979, pp.101

[27] Collin, R.E., *"Field Theory of Guided Waves"* Wiley-IEEE Press, 1991.

[28] Ramesh Garg, Inder Bahl and Maurizio Bozzi, *"Microstrip Lines and Slotlines"* Artech House, 2013.

[29] Nadeem Ashraf, Osama Haraz, M.A.Ashraf and A.Saleh, *"28/38 GHz Dual band millimeter wave SIW array antenna with EBG structures for 5G applications"* IEEE International conference on Information and Communication Technology research (ICTRC), 2015.

[30] A.Alu and N.Engheta, *"Tunneling and growing evanescent envelopes in a pair of cascaded sets of frequency selective surfaces in their band gaps"* Proceedings of the 2004 URSI International Symposium on Electromagnetic Theory, vol. 1, Pisa, Italy, May 2427, 2004, pp. 9092.

[31] J.C.Bose, *"On the rotation of plane of polarisation of electric waves by a twisted structure"* Proc. Roy. Soc., vol. 63, pp. 146152, 1898

[32] Yingpeng Zhang, Dongya Shen, Xingxing Li, Jun Su and Ming Dong, *"A triple-band substrate integrated waveguide antenna based on metamaterials"* IEEE 11th International Symposium on Antennas, Propagation and EM Theory (ISAPE), 2016

[33] V.G.Veselago, *"The electrodynamics of substances with simultaneously negative values of ϵ and μ"* Sov. Phys. Uspekhi, vol. 10, no. 4, pp. 509514, 1968

[34] R.W.Ziolkowski and E.Heyman, *"Wave propagation in media having negative permittivity and permeability"* Phys. Rev. E, vol. 64, no. 5, 056625, Oct. 2001

[35] N.Engheta and R.W.Ziolkowski, *"A positive future for double-negative metamaterials"* IEEE Trans. Microwave Theory Tech., Special Issue on Metamaterial Structures, Phenomena and Applications, vol. 53, no. 4 (part II), pp. 15351556, Apr. 2005

[36] C. Caloz and T. Itoh, *"Microwave applications of novel metamaterials"* Proceedings of the International Conference on Electromagnetics in Advanced Applications, ICEAA03, Torino, Italy, Sept. 2003, pp. 427430

[37] Soumava Mukherjee, Animesh Biswas and Kumar Vaibhav Srivastava, *"Broadband Substrate Integrated Waveguide Cavity-Backed Bow-Tie Slot Antenna"* IEEE Trans. IEEE Antennas and Wireless Propagation Letters, VOL. 13, pp. 11521155, June 2014

[38] C. Caloz and T. Itoh, *"A novel mixed conventional microstrip and composite right/lefthanded backward wave directional coupler with broadband and tight coupling characteristics"* IEEE Microwave Wireless Components Lett., vol. 14, no. 1, p. 3133, Jan. 2004

[39] G.G.V. Eleftheriades, A.K.Iyer, and P.C.Kremer, *"Planar negative refractive index media using periodically L-C loaded transmission lines"* IEEE Trans. Microwave Theory Tech., vol. 50, pp. 27022712, Dec. 2002

[40] A.A.Oliner, *"A periodic-structure negative-refractive-index medium without resonant elements"* paper presented at 2002 IEEE AP-S Int.

Symp./USNC/URSI National Radio Science Meeting, San Antonio, TX, June 1621, URSI Digest, pp.41,2002

[41] A.A.Oliner, Inder Bahl and Maurizio Bozzi, *"A planar negative-refractive-index medium without resonant elements"* in MTT Int. Microwave Symp. (IMS03) Digest, Philadelphia, PA, June 813, 2003

[42] S.Ramo, J.Whinnery and T.Van Duzer, *"Fields and Waves in Communication Electronics"* 2nd ed., Wiley, New York, 1984

[43] H. Raether, *"Surface Plasmons on Smooth and Rough Surfaces and on Gratings"* Springer- Verlag, New York, 1988

[44] G.Broussaud, *"Un nouveau type dantenne de structure plane"* Ann. Radioelectricite, vol. 11, pp. 7088, Jan. 1956

[45] C.N.Hu and C.K.C. Tzuang, *"Analysis and design of large leaky-mode array employing the coupled-mode approach"* IEEE Trans. Microwave Theory Tech., vol. 49, pp. 629636, Apr. 2001

[46] D.Sievenpiperi, *"Forward and backward leaky wave radiation with large effective aperture from an electronically tunable textured surface"* IEEE Trans. Antennas Propag., vol. 53, pp. 236247, Jan. 2005

[47] W.Barnes, T.Priest, S.Kitson and J.Sambles, *"Physical origin of photonic energy gaps in the propagation of surface plasmons on gratings"* Phys. Rev. B, vol. 54, pp. 62276244, Sept. 1996

[48] R.King, D.Thiel and K.Park, *"The synthesis of surface reactance using an artificial dielectric"* IEEE Trans. Antennas Propag., vol. 31, pp. 471476, May 1983.

[49] S.Lee and W.Jones, *"Surface waves on two-dimensional corrugated surfaces"* Radio Sci., vol. 6, pp. 811818, Aug. 1971

[50] R.Elliot, *"On the theory of corrugated plane surfaces"* IRE Trans. Antennas Propag., vol. 2, pp. 7181, Apr. 1954

[51] F.Gardiol, *"Microstrip Circuits"* Wiley, New York, pp. 4850, 1994

[52] C.Y.Cheng and R.W.Ziolkowski, *"Tailoring double negative metamaterial responses to achieve anomalous propagation effects along microstrip transmission line"* IEEE Trans. Microwave Theory Tech., vol. 51, pp. 23062314, Dec. 2003

[53] W.J.Getsinger,*"Microstrip dispersion model"* IEEE Trans. Microwave Theory Tech., vol. MTT-21, pp. 3439, Jan. 1973

[54] Yuandan Dong and Tatsuo Itoh,*"Promising Future of Metamaterials"* IEEE Microwave Magazine, pp- 39-56, March/April 2012

[55] Soumen Pandit, Akhilesh Mohan and Priyadip Ray,*"A low-profile high-gain Substrate-Integrated Waveguide-Slot Antenna with suppressed cross polarization using Metamaterials"* IEEE Antennas and Wireless Propagation Letters, Vol.16,pp-1614-1617, Jan.2017

[56] G.Lovat, P.Burghignoli, F.Capolino, D.R.Jackson and D.R.Walton,*"Analysis of directive radiation from a line source in a metamaterial slab with low permittivity"* IEEE Trans. Antennas and Propagation, Vol.54,pp-1017-1030, March 2006

[57] G.Lovat, P.Burghignoli, F.Capolino and D.R.Jackson, *"Combinations of low/high permittivity and/or pemeability substrates for highly directive planar metamaterial antenna"* Microwave Antennas Propagation, Vol.1, pp-177-183, 2007

[58] Mohammad Mehdi Samadi Taheri, Abdolali Abdipour, Shuai Zhang and G.F.Pedersen , *"Integrated Millimeter-Wave Wideband End-Fire 5G Beam Steerable Array and Low-Frequency 4G LTE Antenna in Mobile Terminals"* IEEE Transactions on Vehicular Technology, Vol. 68 , Issue: 4, April 2019

[59] Jang-Soon Park, Jun-Bong Ko, Heon-Kook Kwon, Byung-Su Kang, Bonghyuk Park and Dongho Kim, *"A tilted combined beam antenna for 5G communications using a 28-GHz band"* IEEE Antennas and Wireless Propagation Letters, Vol. 15, pp.1685 - 1688, Jan 2016

[60] Pang Xingdong, Hong Wei, Yang Tianyang and Li Linsheng, *"Design and implementation of an active multibeam antenna system with 64 RF channels and 256 antenna elements for massive MIMO application in 5G wireless communications"* China Communications, Vol.11, Issue:11, Nov. 2014

[61] Hong Chen, X.Yang, Y.Z.Yin, S.T.Fan and J.J.Wu, *"Triband Planar Monopole Antenna With Compact Radiator for WLAN/WiMAX Applications"* IEEE Antennas and Wireless Propagation Letters, Vol.12, 2013

[62] Y.L.Kuo and K.L.Wong,*"Printed double-T monopole antenna for 2.4/5.2 GHz dual-band WLAN operations"* IEEE Trans. Antennas Propag., vol. 51, no. 9, pp. 21872192, Sep. 2003